

8-2023

Photon Counting Statistics of Classical and Quantum Light Sources

Luis Felipe Morales Bultron
University of Arkansas, Fayetteville

Follow this and additional works at: <https://scholarworks.uark.edu/etd>



Part of the [Quantum Physics Commons](#)

Citation

Morales Bultron, L. F. (2023). Photon Counting Statistics of Classical and Quantum Light Sources. *Graduate Theses and Dissertations* Retrieved from <https://scholarworks.uark.edu/etd/4905>

This Thesis is brought to you for free and open access by ScholarWorks@UARK. It has been accepted for inclusion in Graduate Theses and Dissertations by an authorized administrator of ScholarWorks@UARK. For more information, please contact scholar@uark.edu, uarepos@uark.edu.

Photon Counting Statistics of Classical and Quantum Light Sources

A thesis submitted in partial fulfillment
of the requirements for the degree of
Master of Science in Physics

by

Luis Felipe Morales Bultron
University of Arkansas
Bachelor of Science in Physics and Mathematics, 2019

August 2023
University of Arkansas

This thesis is approved for recommendation to the Graduate Council.

Reeta Vyas, Ph.D.
Thesis Director

Surendra Singh, Ph.D.
Committee Member

William Oliver III, Ph.D.
Committee Member

Pradeep Kumar, Ph.D.
Committee Member

Abstract

Multiple sources of light, including coherent light, thermal light, light from a degenerate parametric oscillation and resonance fluorescence from a two level coherently driven atom are considered for the analysis of their wait time statistics. We include the second order normalized correlation function and Mandel's Q parameter for brief discussion. A general framework to analyze the generalized conditional and unconditional wait time distributions is also obtained in order to understand the photo-count statistics of the light sources included in this work. Average and variance of wait times with respect to both unconditional and conditional wait time distribution are also obtained and briefly discussed.

Acknowledgements

I am deeply grateful to my advisers, Professors Reeta Vyas and Surendra P. Singh. They are a mother and a father figure to me and to many others, not only academically but also in life. They truly are educators, and I mean that in the whole sense of the word. I will always be thankful for their unbounded patience, understanding and their will to see me (and every student they have had) succeed as a person and as a scientist. To my parents, that even though are far away, they motivated me from a distance, always supported and believed in my capacity. To Professor William Oliver III, whose help in everything made things work and fall into their respective place. Without him, I also could not have done much. I am specially indebted to Professor Pradeep Kumar for our many discussions in physics and for his multiple advice in how to become and think like an actual physicist. There are not enough words in any language I know to express how grateful I am to these people, but I can only say, *thank you*.

Table of Contents

1	Introduction	1
2	Background	4
2.1	Quantization of the Electromagnetic Field and its Point Process Description	4
2.2	Coherence Functions for The Quantized Field	6
2.3	Generating Function and Factorial Moments of a Photon Sequence Process .	10
2.4	Mandel's Q Parameter	11
2.5	Generalized Wait Time Distributions	12
2.6	Unconditional and Conditional Average and Variance of Wait Time τ of the n th Photoelectric Detection	19
3	Counting statistics of Coherent Light	21
4	Photon Counting Statistics of Thermal Light	23
4.1	Small \bar{n} Limit	25
4.2	Large \bar{n} Limit	26
5	Photon Counting Statistics of the Degenerate Parametric Oscillator	31
5.1	Description of the DPO	31
5.2	Small Mean Cavity Photon Number \bar{n}	34
5.3	Large Mean Photon Number $\bar{n} \gg 1$	38
5.4	Effect of Non-Unit Detection Efficiency	43
6	Photon Counting Statistics of Resonance Fluorescence of Two Level Atom	45
6.1	Unit Detection Efficiency $\eta = 1$	48
6.2	Non-Unit Detection Efficiency Effect	52
7	Summary	60
7.1	Conclusion	60

7.2 Future Work	62
Bibliography	64

List of Figures

Figure 2.1:	Graphical representation of a randomly distributed (a), bunched (b), and anti-bunched (c) photon sequence.	9
Figure 4.1:	Comparison of the exact (solid black curves) and approximate (dashed black curves) expressions for $P_n(\tau)$ and $w_n(\tau)$ for $n = 1-3$ thermal photons for small $\bar{n} = 0.01$	24
Figure 4.2:	Comparison of the exact (solid black curves) and approximate (dashed black curves) expressions for $P_n(\tau)$ and $w_n(\tau)$ for $n = 1-3$ thermal photons for large $\bar{n} = 10$	24
Figure 4.3:	Unconditional average and variance of wait time τ for the photodetections $n = 1 - 4$. We do not include averages and variances with respect to w_n since the are given in terms of the averages and variances with respect to P_n	29
Figure 5.1:	Exact curves (solid black) and approximations (dashed black curves) for $P_n(\tau)$ and $w_n(\tau)$ for the case that $\bar{n} \ll 1$ for DPO $n = 1-3$ photons.	37
Figure 5.2:	Exact curves for $P_n(\tau)$ and $w_n(\tau)$ for squeezed light from a DPO for $n = 1-3$ compared with approximate expressions (dashed curves) given by Eqs. (5.28) and (5.30) for $\bar{n} = 10$	37

Figure 5.3:	Unconditional average and variance of wait time τ for the photodetections $n = 1 - 4$ for the DPO case. As was the case for the plots for curves for thermal light we do not include averages and variances with respect to w_n	41
Figure 5.4:	Effect of the non-unit detection efficiency. Exact curves for $P_n(\tau)$ and $w_n(\tau)$ for squeezed light from a DPO for $n = 1-3$ compared with approximate expressions (dashed curves) given by Eqs. (5.37)-(5.40) for $\bar{n} = 0.01$	42
Figure 6.1:	$w_n(\tau)$ and $P_n(\tau)$ for small ($\Omega/\beta = 0.2\sqrt{2}$ sub-figures (a)-(b)), resonant ($\Omega/\beta = 1$ sub-figures (c)-(d)), and large ($\Omega/\beta = 10\sqrt{2}$, sub-figures (e)-(f)) driving fields for $n = 1 - 4$. The dashed curves in sub-figures (e) and (f) represent large field approximations, see Eq.(6.18).	51
Figure 6.2:	Effect of the non-unit detection efficiency on unconditional waiting time distributions for resonance fluorescence for $n = 1 - 4$. The distribution approach the coherent limit as η decreases, this can be seen through figures (a)-(e) where the dashed curve represents coherent light.	54
Figure 6.3:	Conditional and Unconditional variance of wait time τ for the photodetections $n = 1 - 4$ for resonance fluorescence. Notice as in the large field limit, each variance approaches its corresponding n value.	58

Chapter 1

Introduction

Photon statistics is a discipline that lies at the heart of theoretical and experimental quantum optics. Results obtained in the general field theoretical framework for photon statistics provide guidance for experiments such as the Hanbury Brown-Twiss interferometry, entanglement of photons, phase interference, etc. [1–4]. Experiments that rely on photon coincidence measurement are used to test theoretical results that have been obtained through assumptions about the possible quantum statistical description of the electromagnetic field; especially optical fields that are useful and applicable to/from lasers, optical masers, optical cavities, interferometers, and other useful optical fields. Photon statistics is particularly an interesting sub-branch of quantum optics since from the experimental point of view, to accurately measure photon correlations, one requires a high degree of accuracy which means one must have access sufficiently efficient detectors if one wishes to recreate a photon sequence via photoelectric pulse creation. The challenge, however, is that photodetectors do not have perfect efficiency of detection. Photodetectors rely on the fact that when they detect a photon from a beam of photons the photon is converted to a voltage pulse. This may not always happen since the atomic media that comprises these instruments have imperfections and will not always recreate a voltage pulse sequence equivalent to that of the photo-emission sequence incident on the detector. Realistically speaking, one is only able to measure the photoelectric or voltage pulses.

In the present work, we delve more into how one can categorize sources that produce photon sequences and how to study the temporal behavior of these photon sequences. However, before we start, we make a few remarks about photons. Light is fully described by a set of equations known as Maxwell’s equations, in vacuum or in a certain medium. Once one combines the framework of quantum mechanics and electrodynamics, the electromagnetic wave fields described by Maxwell equations can be thought of “particles” or wave packets

called photons. Photons are fundamental in nature. They are the fundamental carriers of information across space and time. A vast majority of today's communication systems rely on reliable exchange of photons. There are of course other types of waves (acoustic, spin, phonons, etc.) that are useful for communication, but photons are of high interest here. For instance, high speed internet, photonic quantum computing, radio transmissions, etc. are a few of the most important current applications of photons in communication. Thus, knowing fundamental properties of photons such as their phase, polarization, energy, and other of their spatial and temporal as well as statistical properties will certainly become handy if one is to build and improve communications systems that rely heavily in optical components.

One can understand photons from the theoretical and mathematical point of view due to quantum electrodynamics and quantum field theory which in combination with optics and quantum mechanics provide the full framework of quantum optics. In our current work, we will not study individual photons. We will study their collective properties. For the present thesis, let us consider that position is fixed and thus our detectors are at fixed points in space. So, our only concern henceforth is with time, the temporal-statistical properties of photon sequences to be more exact.

Any beam of light contains photons and consequently these photon sequences can be approximately described by a mathematical tool called time series. Such times series can be continuous or discrete depending on the properties and characteristics one wishes to observe. Usually a photon sequence process follows a stochastic point process [5, 12]

Understanding and analyzing the statistical properties of photon sequences generated from a specific material, physical process, or other light sources represents an essential tool to unveil the internal dynamics that govern all these photon-emitting sources. Based on the experimental predictions and theoretical derived results, one can implement a protocol for reliably categorize the nature of a light source as quantum or classical [1, 5–8] .

The thesis is organized as follows. The present chapter, Chapter 1, is of course the introduction. Chapter 2, the background, introduces the concept of quantized electromagnetic

field and its use in correlation functions essential for quantum optics. Other statistical quantities of vital importance such as generating functions, moments of the photon sequence, Mandel's Q parameter, photon count probabilities, and generalized wait time distributions (unconditional and conditional) are derived and defined. In Chapter 3, we use the formalism derived in Chapter 2 to illustrate the case of coherent light and lay ground for comparing the rest of other light sources discussed in the thesis. In Chapter 4, generalized wait time statistics of thermal light sources are analyzed and compared to a coherent photon sequence. Chapter 5 introduces squeezed light from a degenerate parametric oscillator (DPO) and its general statistical description. A section of chapter 5 is devoted to the effect of non-unit detection efficiency of light from a DPO. Lastly, Chapter 6 covers the generalized wait time statistics for resonance fluorescence of coherently driven two level atom and the case of anti-bunching of its photon sequence as well as exact generalized expressions for the non-unit detection efficiency regime. The conclusion and future work section of Chapter 7 summarizes the main points and the research we will continue to do.

Chapter 2

Background

2.1 Quantization of the Electromagnetic Field and its Point Process Description

All electromagnetic fields in vacuum or in interaction with matter can be represented by the operators $\hat{\mathbf{E}}(\mathbf{r},t)$ and $\hat{\mathbf{B}}(\mathbf{r},t)$, the electric and magnetic field observables respectively. Both the electric and magnetic fields satisfy Maxwell's equations. This is a set of four linear partial differential equations that can be solved subject to boundary conditions, if present, or solved in vacuum. There are two widely used descriptions of the electromagnetic field, the classical and quantum mechanical. Within the classical framework, Maxwell's equations can be solved to produce solutions in terms of sums of plane waves with a certain polarization which can also be used to treat photons classically. With respect to the other case, the quantum mechanical framework, the solutions of these equations are assumed to be vector valued field operators whose Fourier expansion is in terms of annihilation and creation operators—the same operators that are used for the description of the quantum mechanical harmonic oscillator. In the case of electromagnetic waves, these operators are associated to a wave vector \mathbf{k} . We are interested in the electric part of the field since the magnetic field can be mathematically obtained from the electric field operator and the electric field is directly measurable in experiments [1, 2, 9]. The most general electric field quantum operator can be written as

$$\hat{\mathbf{E}}(\mathbf{r}, t) = i \sum_{\mathbf{k}, s} \left(\frac{\hbar \omega(\mathbf{k})}{2\epsilon_0 V} \right)^{1/2} \mathbf{e}_{\mathbf{k}, s} \hat{a}_{\mathbf{k}, s}(t) e^{i\mathbf{k} \cdot \mathbf{r}} + c.c. \quad (2.1)$$

In Eq. (2.1), \mathbf{k} is the wave vector, $\mathbf{e}_{\mathbf{k}, s}$ is the polarization vector and s denotes which polarization vector, V is the quantization volume (if the quantum field is to be confined in an optical cavity then V equals this confinement volume), $\omega(\mathbf{k})$ is the frequency of the field, $\hat{a}_{\mathbf{k}, s}(t)$ is the time dependent annihilation operator and its complex conjugate transpose is the creation operator and $c.c$ denotes the complex transpose conjugate. In the case that the

wave vector \mathbf{k} is continuous one makes the transform $\sum_{\mathbf{k}} \rightarrow \int_V d^3\mathbf{k}g(\mathbf{k})$ where $g(\mathbf{k})$ is some weight function. For convenience, Eq. (2.1) may be redefine as

$$\hat{\mathbf{E}}(\mathbf{r}, t) = \hat{\mathbf{E}}^{(-)}(\mathbf{r}, t) + \hat{\mathbf{E}}^{(+)}(\mathbf{r}, t) \quad (2.2)$$

where the $(-)$ and $(+)$ are known as the negative and positive frequency components of the electric field and they correspond to the creation and annihilation operators respectively [1,9].

For the sake of briefly introducing the theory of coherence, common assumptions in the literature are to assume that the field is a single mode plane wave with wavelength far larger than that of atomic distances of the medium the field interact with; this medium is usually taken to be the material for which the photodetector is made of. The field is incident on photodetectors placed in fixed positions so the symbol \mathbf{r} in Eq. (2.2) becomes redundant, one just drops it. In this case the negative frequency part of the electric field reduces to

$$\hat{E}^{(-)}(t) = iC\hat{a}(t) \quad (2.3)$$

where the constant $C = (\hbar\omega/2\varepsilon_0V)^{1/2}$. In Eq. (2.3) we have not written the negative frequency part of the electric field bold font which means is a vector but instead we have dropped that notation. This is the case since we are not interested in the vectorial properties of the electric field which stem from the polarization vector associated to it. By means that are far beyond the scope of this thesis and whose framework is extremely well developed, see for example Refs. [1, 2, 6, 9], we define the intensity or photon-flux operators as

$$\hat{I}(t) = \hat{E}^{(-)}(t)\hat{E}^{(+)}(t) = C^2\hat{a}^\dagger(t)\hat{a}(t) = C^2\hat{n}(t). \quad (2.4)$$

We remark that the constant C is of no relevance to our discussion. The specific order of the negative and positive frequency components of the electric field operator in the equation above has been chosen since one is concerned with theory and experiments related to photodetections, thus annihilation of a photon is succeeded by the creation of another photon (as read from right to left), all to conserve energy. This specific rule, in an arbitrary product

string of creation and annihilation operators, of situating the creation operators on the far left and the annihilation operators on the far right is known as normal ordering [6, 9].

2.2 Coherence Functions for The Quantized Field

In the previous discussion, we have defined an operator known in the literature as the number operator, $\hat{n}(t) = \hat{a}^\dagger(t)\hat{a}(t)$. Consider now two photo-detection events at two different times t and $t + \tau$ given by $\hat{I}(t)$ and $\hat{I}(t + \tau)$. One can then ask how the two events statistically related by calculating the covariance of \hat{I} at these two times, t and $t + \tau$. The averaged two-point correlation function or also known in optics as the second order coherence function is defined as

$$\begin{aligned} g^{(2)}(t, t + \tau) &= 1 + \frac{Cov[\mathcal{T} : \hat{I}(t)\hat{I}(t + \tau) :]}{\langle : \hat{I}(t) : \rangle \langle : \hat{I}(t + \tau) : \rangle} \\ &= \frac{\langle \mathcal{T} : \hat{I}(t + \tau)\hat{I}(t) : \rangle}{\langle : \hat{I}(t + \tau) : \rangle \langle : \hat{I}(t) : \rangle} = \frac{\langle : \hat{n}(t + \tau)\hat{n}(t) : \rangle}{\langle \hat{n}(t) \rangle \langle \hat{n}(t + \tau) \rangle} \end{aligned} \quad (2.5)$$

where Cov is the covariance of the variable \hat{I} , \mathcal{T} is time ordering, $: \dots :$ denotes normal ordering of the creation and annihilation operators and $\langle \dots \rangle$ is a quantum mechanical average.

It is also possible to define $g^{(1)}(t, t + \tau)$, the first order coherence function as $g^{(1)}(t, t + \tau) = \frac{\langle \hat{a}^\dagger(t)\hat{a}(t + \tau) \rangle}{\sqrt{\langle \hat{n}(t) \rangle \langle \hat{n}(t + \tau) \rangle}}$. Physically speaking, $g^{(2)}$ can be interpreted as a conditional probability that a photon detection at $t + \tau$ is conditioned upon a photon detection at time t . The physical meaning of $g^{(1)}$ is related to the interference patterns in a Young's Double Slit experiment. This is so, since the visibility of the fringe pattern is proportional to $|g^{(1)}|$ [4].

One can define an n th order coherence function for the intensity or photon-flux of the electric field. For times $t_1 < t_2 < \dots < t_n$ the n th order coherence is define as

$$g^{(n)}(t_1, t_2, \dots, t_n) = \frac{\langle \mathcal{T} : \hat{I}(t_n) \cdot \dots \cdot \hat{I}(t_1) : \rangle}{\prod_{j=1}^n \langle : \hat{I}(t_j) : \rangle}. \quad (2.6)$$

The interpretation of $g^{(n)}$ is similar to that of $g^{(2)}$, except that now, each event that happens at time t_i is conditioned upon the event that happens at time t_{i-1} [1, 6, 9].

To further proceed with our analysis, it is important to recognize that is possible to drop the hats on photon-flux operators, \hat{I} , since creation and annihilation operators of the quantum field can be mapped to a corresponding set of stochastic variables described within the appropriate use of generalized probability distributions [1, 4, 10, 11].

Let us briefly make a digression to stochastic analysis. Consider a stochastic process described by the set of variables $I = \{I_1(t), \dots, I_N(t)\}$. For a fix time t_0 , $I_j(t_0)$, for any $j = \{1, \dots, N\}$ denotes a random variable. The indexing j for fix time denotes a possible realization of the process. For example, $I_j(t)$ is a sample function or a realization of the process and it evolves in time.

We can think of the set $\{I_1(t), \dots, I_N(t)\}$ as an ensemble of events described by their respective variable, time. Usually, to understand a random process, a common practice is to define the concept of “ergodicity.” An Ergodic process is that which averages over an ensemble (possible realizations of the stochastic process) is the same as averages taken over time [12]. During this thesis we consider photon counting events as Ergodic processes [5]. An important concept we are going to use is that of wide-sense stationarity. Let us define what a stationary process is. A signal, a time series, or a stochastic process that is described by the variable $I(t)$ is said to be stationary in the wide-sense if and only if for any two different times t and t' , the expectation and correlation of the signal satisfy the following

$$\mathbb{E}[I(t)] = \mathbb{E}[I(t')], \quad (2.7)$$

$$\Gamma(t, t') = \mathbb{E}[I(t')I(t)] = \Gamma(|t' - t|), \quad (2.8)$$

i.e the correlation function Γ only depends on the difference of times t' and t . We have also used the notation \mathbb{E} for expectation value either over ensembles or time, but in the context of this thesis it means the same as a quantum mechanical expectation $\langle \dots \rangle$.

Given our digression above about signals, we may assume that the signals treated here are stationary. However, in the current chapter we will derive expressions for photon sequences that are not necessarily stationary. The photon sequences treated in Chapters 3, 4, 5 and 6

will be considered stationary.

Within the framework of quantum optics and the theory of coherence, it is possible to define a set of equality and inequalities that provide a way of categorization for a quantum optical field into classical or quantum mechanical. However, before we introduce this formalism, we must introduce the concept of coherent states of the electromagnetic field. This is our reference point, and we will continuously use it throughout this thesis as means for checking and comparing our results. First, let us point out that coherent states are those states that are right eigenstates of the annihilation operator \hat{a} [4] and their occupation number probability, in the number state basis (this basis comprises the eigenstates of the number operator, \hat{n}), is given by a Poisson distribution [1, 4].

As it turns out, the theoretical framework backed by vast experimental results in quantum optics lead one to be able to categorize coherent light as having uniform intensity with respect to time [1], as long as the signal has a coherence time. From the point of view of statistics, the photon-flux operator for a coherent field is described as a stationary Poisson point process. Consequently, the second order correlation, or any order of the correlation for the field intensity satisfies $g^{(n)}(t_1, t_2, \dots, t_n) = 1$. We shall use this as our reference for classifying other sources of light.

In order to present reasonable results, we henceforth restrict our discussion to the second order correlation function to define and explain what inequalities a classical electromagnetic field must satisfy. These set of inequalities can be used to measure and test the result of quantum electrodynamics. A field that is described in the phase space representation by classical or non classical probabilities [10, 11] is said to be a coherent field if its second order correlation function satisfies [13]

$$g^{(2)}(t, 0) \geq 1, \tag{2.9}$$

$$g^{(2)}(t, 0) \geq g^{(2)}(t, \tau), \tag{2.10}$$

$$|g^{(2)}(t, 0) - 1| \geq |g^{(2)}(t, \tau) - 1|. \tag{2.11}$$

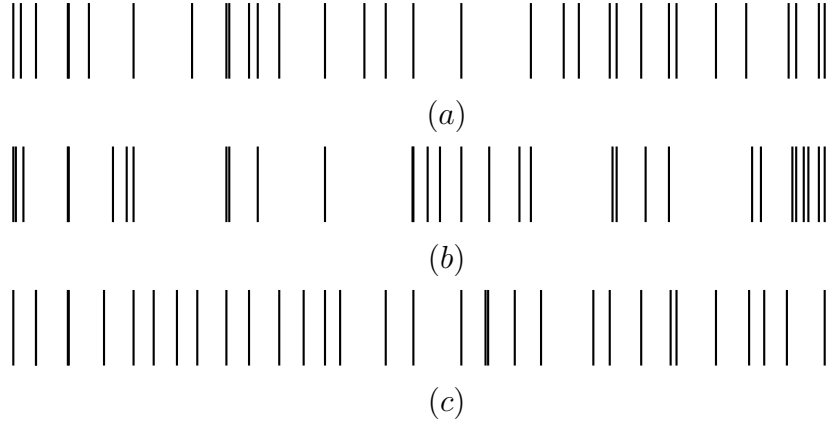


Figure 2.1: Graphical representation of a randomly distributed (a), bunched (b), and anti-bunched (c) photon sequence.

Violation of these inequalities imply the quantum nature of the light field [13]. Notice that by using Schwartz inequalities, one can prove that it is always the case that $0 \leq g^{(2)}(t, 0)$, at least for a coherent field that has classical probabilistic description. Furthermore, using the criteria for the second order intensity correlation function, we define the following conditions:

1. A photon sequence is said to be randomly distributed if $g^{(2)}(t, 0) = 1$.
2. A photon sequence is said to be bunched if $g^{(2)}(t, 0) \geq 1$.
3. A photon sequence is said to be anti-bunched if $0 \leq g^{(2)}(t, 0) < 1$.

The above conditions refer to a particular grouping of photons temporally. We illustrate this in Fig. 2.1.

In addition to the above conditions, we must remark that even though light fields such as squeezed states of the electromagnetic spectrum satisfy the above inequalities for $g^{(2)}$, Eqs. (2.9)-(2.11), it is still a type of light that requires a fully quantum mechanical treatment to be accurately described [1, 4, 10, 14, 15]. Thus, the above inequalities are one of many criteria to expose the true nature, classical or quantum, of the electromagnetic field. Another important criterion is that of the Heisenberg uncertainty relation. One last remark, notice that all orders of the intensity correlation functions are independent of the quantum efficiency of the detectors. This allows experimental measurements of any degree of coherence of a light field

even if the detection efficiency is not ideal [1, 2]. However, if enough photons are deleted from a photon sequence due to non-ideal detection efficiency, more experimental trials are required for one to be able to recreate faithful photon correlation statistics.

2.3 Generating Function and Factorial Moments of a Photon Sequence Process

We now define the generating function G for a light beam that is described by the photon-flux operator $\hat{I}(t)$. For the moment, we do not make any assumptions about the light beam being stationary. We will first obtain general expressions and offer understanding for any photon sequence. For times $t_1 = t$ and $t_2 = t + \tau$ we define the generating function to be

$$G(s, t_1, t_2) = \left\langle \mathcal{T} : \exp(-s\eta\hat{U}(t_1, t_2)) : \right\rangle. \quad (2.12)$$

Where the new parameter introduced, s , serves as means for computing other useful statistical quantities. We have also defined the operator $\hat{U}(t_1, t_2)$, this is the integrated photon-flux or integrated intensity and is given by

$$\hat{U}(t_1, t_2) = \int_{t_1}^{t_2} \hat{I}(t) dt. \quad (2.13)$$

Notice that $G(s, t_1, t_2)$ is the probability that not photoelectric detection occurs in the interval of time $[t_1, t_2]$. An equally essential quantity in our studies is the probability that n photo-electron counts have been recorded in the interval $[t_1, t_2]$, the expression is defined to be

$$\begin{aligned} p(n, t_1, t_2) &= \frac{(-1)^n}{n!} \frac{\partial^n}{\partial s^n} G(s, t_1, t_2) \Big|_{s=1} \\ &= \left\langle \mathcal{T} : \frac{[\eta\hat{U}(t_1, t_2)]^n}{n!} \exp(-s\eta\hat{U}(t_1, t_2)) : \right\rangle. \end{aligned} \quad (2.14)$$

The derivation will not be discussed here however Ref. [16] has all the remarks about Eq. (2.14).

Furthermore, it is important to realize that $G(s, t_1, t_2)$ is the basis for the majority of the

arguments and computations in this thesis. Such generating function becomes essential in the calculation of the factorial moments of the light field [1]. We define the factorial moments of a photon sequence described by the generating function G to be

$$\langle m^{(r)}(t_1, t_2) \rangle = (-1)^r \frac{\partial^r}{\partial s^r} G(s, t_1, t_2) \Big|_{s=0}. \quad (2.15)$$

Where r is a positive integer. Now, as $r \geq 2$ the calculation of the factorial moments becomes particularly involved depending on the case one is studying. For example, briefly consider $\langle m^{(2)} \rangle$, the second order factorial moment. Its formula is given by

$$\begin{aligned} \langle m^{(2)}(t, t + \tau) \rangle &= \eta^2 \int_t^{t+\tau} dt_2 \int_t^{t+\tau} dt_1 \langle \hat{I}(t_2) \hat{I}(t_1) \rangle \\ &= \eta^2 \int_0^\tau dt_2 \int_0^\tau dt_1 \langle \hat{I}(t_2 + t) \hat{I}(t_1 + t) \rangle. \end{aligned} \quad (2.16)$$

In principle, calculation of $\langle \hat{I}(t_2 + t) \hat{I}(t_1 + t) \rangle$ follows the exact same algorithm used to calculate the second order correlation function $g^{(2)}$ only in this case one replaces different time variables and integrate the final expression. Since we have mentioned $\langle m^{(2)} \rangle$, we consider proper the introduction of Mandel's Q parameter in the following section and also some of its implications on the departure of the statistics for which a photon sequence is characterized.

2.4 Mandel's Q Parameter

Mandel's Q parameter is an important measure about the statistical properties of a light beam. One can understand the departure of the statistical distributions from Poissonian statistics by computing Mandel's Q parameter [17]. The Q parameter is defined as

$$Q(t_1, t_2) = \frac{\langle m^{(2)}(t_1, t_2) \rangle - \langle m^{(1)}(t_1, t_2) \rangle^2}{\langle m^{(1)}(t_1, t_2) \rangle} = \frac{\int_{t_1}^{t_2} dt' \int_{t_1}^{t_2} dt'' \langle \hat{I}(t') \rangle \langle \hat{I}(t'') \rangle (g^{(2)}(t', t'') - 1)}{\int_{t_1}^{t_2} dt' \langle \hat{I}(t') \rangle}. \quad (2.17)$$

If the photon sequence is stationary, i.e $\langle \hat{I}(t_1) \rangle = \langle \hat{I}(t_2) \rangle$ and $g^{(2)}(t_1, t_2) = g^{(2)}(|t_2 - t_1|)$, i.e correlation of the photon-flux operator only depends on the difference of time $|t_2 - t_1|$, the

explicit form for Q [14, 17, 18] is then

$$\begin{aligned} Q(t_1, t_2) &= \frac{\langle m^{(1)} \rangle}{(t_2 - t_1)^2} \int_{t_1}^{t_2} dt' \int_{t_1}^{t_2} dt'' (g^{(2)}(t', t'') - 1) \\ &= \frac{2\langle m^{(1)} \rangle}{|t_2 - t_1|} \int_0^{|t_2 - t_1|} \left[1 - \frac{t'}{|t_2 - t_1|} \right] (g^{(2)}(t') - 1) dt' = Q(|t_2 - t_1|). \end{aligned} \quad (2.18)$$

Given Eq. (2.17) and (2.18), one can establish yet another set of equality and inequalities similar to those given for $g^{(2)}$. However, the following conditions on Mandel's Q parameter then establish what type of statistics a certain photon sequence obeys. They are given as follows:

1. if $Q = 0$, then a photon sequence is said to follow Poissonian statistics.
2. if $Q > 0$, then a photon sequence follows super-Poissonian statistics.
3. If $Q < 0$, then a photon sequence is said to follow sub-Poissonian statistics.

For some photon sequences, we remark that it is possible that anti-bunching can be accompanied by super-Poissonian or sub-Poissonian statistics as it may just as well be the case with bunching [1, 17, 18].

2.5 Generalized Wait Time Distributions

A large portion of this thesis is devoted to the generalized unconditional and conditional wait time distributions of the n th photoelectric detection from a photon sequence. Our ultimate aim with this section is to first introduce the case for both wait time distributions for the *first* photoelectric detection and then define the generalized $P_n(t_1, t_2)$ and $w_n(t_2 - t_1|t_1)$, unconditional and conditional wait time distributions. Let us introduce the following probability distribution known as the r -fold photo-electron count probability. Consider the interval of time $[t_0 = t, t_r = t + \tau]$. It is convenient to set $t = t_0 < t_1 < \dots < t_r = t + \tau$ (where t_0, \dots, t_r is a partition of the interval of time $[t, t + \tau]$) then the photo-electron count

probability is given by [19]

$$p^{(r)}(n_1, t_0, t_1; \dots; n_r, t_{r-1}, t_r) = \left\langle : \prod_{j=1}^r \frac{[\eta \hat{U}(t_{j-1}, t_j)]^{n_j}}{n_j!} \exp(-\eta \hat{U}(t_{j-1}, t_j)) : \right\rangle. \quad (2.19)$$

The above probability is interpreted as the probability of detecting n_j photoelectric pulses in each interval of time $[t_{j-1}, t_j]$. In what follows we only derive $w_1(t_2 - t_1|t_1)$ and omit the derivation of $P_1(t_1, t_2)$. We omit the derivation of $P_1(t_1, t_2)$ since we are also considering the general case. Consider now the following scenario. First, a photoelectric detection is recorded in the interval $[t_1 - \delta t_1, t_1]$, no photoelectric detection is recorded in the interval $[t_1, t_2]$ and another photoelectric detection is recorded in the interval $[t_2, t_2 + \delta t_2]$. In the previous, we have chosen both δt_1 and δt_2 to be positive and very small real numbers. One can translate this situation using the $r = 3$ r -fold photoelectric pulse count probability, Eq. (2.19), which leads to

$$p^{(3)}(1, t_1 - \delta t_1, t_1; 0, t_1, t_2; 1, t_2, t_2 + \delta t_2) = \eta^2 \left\langle : \hat{U}(t_2, t_2 + \delta t_2) e^{-\eta \int_{t_1}^{t_2} \hat{I}(t) dt} \hat{U}(t_1 - \delta t_1, t_1) : \right\rangle.$$

The interpretation of the 3 fold probability for the above describes the joint probability that two photoelectric pulse detections have happened in the whole interval $[t_1, t_2]$. However, we are interested in the conditional probability, $w(t_2 - t_1|t_1)$, that a photoelectric detection at t_2 is conditioned upon a photoelectric pulse detection recorded at time t_1 after a time $t_2 - t_1$ elapses. By this interpretation we then have

$$\begin{aligned} w(t_2 - t_1|t_1) &= \lim_{\delta t_1, \delta t_2 \rightarrow 0} \frac{p^{(3)}(1, t_1 - \delta t_1, t_1; 0, t_1, t_2; 1, t_2, t_2 + \delta t_2)}{\delta t_2 p^{(1)}(1, t_1 - \delta t_1, t_1)} \\ &= \frac{\eta \left\langle : \hat{I}(t_2) \exp[-\eta \int_{t_1}^{t_2} \hat{I}(t) dt] \hat{I}(t_1) : \right\rangle}{\langle : \hat{I}(t_1) : \rangle}. \end{aligned} \quad (2.20)$$

The derivation of $P(t_1, t_2)$ and $w(t_2 - t_1|t_1)$ are also well described in detail in [8, 19]. However, the process and algorithm for which $w(t_2 - t_1|t_1)$ is obtained is so essential that we feel that in order to understand generalized wait time distributions, we replicate the derivation here once more. With the above remarks, we are now moving towards the generalized wait

time distributions, unconditional and conditional. We now define the generalized unconditional wait time distribution as $P_n(t_1, t_2)$ and $w_n(|t_2 - t_1| | t_1)$ respectively. Suppose one starts counting at an arbitrary time interval $[t_1 - \delta t_1, t_1]$ without having to detect a photon, i.e the counting process commences arbitrarily in time, then in order to record a n th photoelectric detection after a time $|t_2 - t_1|$ has elapsed, $n - 1$ photoelectric deection events must have taken place. One does not know how and when exactly these $n - 1$ events happened; however, it is important that they indeed happen before the n th photoelectric detection could be ever recorded. After time $|t_2 - t_1|$ elapses, the n th photoelectric pulse is detected in the interval of time $[t_2, t_2 + \delta t_2]$. We can once more translate the just-described scenario mathematically in terms of the r -fold probability for $r = 3$ as follows

$$\begin{aligned} P_n(t_1, t_2) &= \lim_{\delta t_1, \delta t_2 \rightarrow 0} \frac{p^{(3)}(0, t_1 - \delta t_1, t_1; n - 1, t_1, t_2; 1, t_2, t_2 + \delta t_2)}{\delta t_2} \\ &= \left\langle : \eta \hat{I}(t_2) \frac{[\eta \hat{U}(t_1, t_2)]^{n-1}}{(n-1)!} \exp[-\eta \int_{t_1}^{t_2} \hat{I}(t) dt] : \right\rangle. \end{aligned} \quad (2.21)$$

Similarly, the physical considerations for $w_n(t_2 - t_1 | t_1)$ is that instead of commencing the counting process at an arbitrary time interval $[t_1 - \delta t_1, t_1]$ with not photoelectric detection, we required that there be a photoelectric detection in this time interval. And we require that the n th photoelectric detection is conditioned upon such photoelectric detection at time interval $[t_1 - \delta t_1, t_1]$, then we must divide the $r = 3$ r-fold probability used for the derivation of $P_n(t_1, t_2)$ by the probability $p^{(1)}(1, t_1 - \delta t_1, t_1)$ of making a photoelectric detection in this interval of time. In summary, we have that

$$\begin{aligned} w_n(t_2 - t_1 | t_1) &= \lim_{\delta t_1, \delta t_2 \rightarrow 0} \frac{p^{(3)}(1, t_1 - \delta t_1, t_1; n - 1, t_1, t_2; 1, t_2, t_2 + \delta t_2)}{\delta t_2 p^{(1)}(1, t_1 - \delta t_1, t_1)} \\ &= \eta \frac{\left\langle : \hat{I}(t_2) \frac{[\eta \hat{U}(t_1, t_2)]^{n-1}}{(n-1)!} \exp[-\eta \int_{t_1}^{t_2} \hat{I}(t) dt] \hat{I}(t_1) : \right\rangle}{\langle : \hat{I}(t_1) : \rangle}. \end{aligned} \quad (2.22)$$

The above arguments are long for both wait time distributions. However, they are essential in their derivation and we remark that the physical understanding for this arguments is essential in moving forward.

We now present alternative definitions of $P_n(t_1, t_2)$ and $w_n(t_2 - t_1|t_1)$ that do not rely on physical grounds, rather they are convenient for calculating and obtaining analytic expressions for the systems light sources presented in future chapters.

Recall the definition of generating function given in Eq. (2.12). The unconditional and conditional wait time distributions can be expressed in terms of the generating function as follows:

$$P_n(t_1, t_2) = -\frac{(-1)^{n-1}}{(n-1)!} \left[\frac{\partial^{n-1}}{\partial s^{n-1}} \frac{1}{s} \frac{\partial}{\partial t_2} G(s, t_1, t_2) \right] \Big|_{s=1}, \quad (2.23)$$

$$w_n(t_2 - t_1, t_1) = \frac{1}{\eta \langle : \hat{I}(t_1) : \rangle} \frac{(-1)^{n-1}}{(n-1)!} \left[\frac{\partial^{n-1}}{\partial s^{n-1}} \frac{1}{s^2} \frac{\partial^2}{\partial t_2 \partial t_1} G(s, t_1, t_2) \right] \Big|_{s=1}. \quad (2.24)$$

Notice from Eq. (2.23) and Eq. (2.24) when $n = 1$ the equations reduce to the well-known expressions for $P(t_1, t_2)$ and $w(t_2 - t_1|t_1)$. Furthermore, it is also possible to define recurrence relations for Eq. (2.23) and Eq. (2.24) in terms of the photoelectric count probability, Eq. (2.14). $P_n(t_1, t_2)$ satisfies the following recurrence relation

$$\frac{\partial}{\partial t_2} p(n, t_1, t_2) = P_n(t_1, t_2) - P_{n+1}(t_1, t_2). \quad (2.25)$$

With $P_0(t_1, t_2) = 0$, the recurrence relation has solution

$$P_n(t_1, t_2) = -\frac{\partial}{\partial t_2} \left[\sum_{k=0}^{n-1} p(k, t_1, t_2) \right]. \quad (2.26)$$

In a similar manner, $w_n(t_2 - t_1|t_1)$ satisfies another recurrence,

$$\frac{1}{\eta \langle : \hat{I}(t_1) : \rangle} \frac{\partial^2}{\partial t_2 \partial t_1} p(n, t_1, t_2) = w_{n-1}(t_2 - t_1|t_1) - 2w_n(t_2 - t_1|t_1) + w_{n+1}(t_2 - t_1|t_1). \quad (2.27)$$

Along with $w_n(t_2 - t_1|t_1) = 0$ for any integer $n \leq 0$, the above recurrence is easily shown to satisfy

$$w_n(t_2 - t_1|t_1) = \frac{1}{\eta \langle : \hat{I}(t_1) : \rangle} \frac{\partial^2}{\partial t_2 \partial t_1} \left[\sum_{k=0}^{n-1} (n-k) p(k, t_1, t_2) \right]. \quad (2.28)$$

A further inspection, shows that the above recurrence relations and conditions on $P_n(t_1, t_2)$ and $w_n(t_2 - t_1|t_1)$ provide yet another recurrence relation for $P_n(t_1, t_2)$ and $w_n(t_2 - t_1|t_1)$

[20–22]

$$\frac{1}{\eta \langle : \hat{I}(t_1) : \rangle} \frac{\partial}{\partial t_1} P_n(t_1, t_2) = w_{n-1}(t_2 - t_1 | t_1) - w_n(t_2 - t_1 | t_1) \quad (2.29)$$

with solution

$$w_n(t_2 - t_1 | t_1) = -\frac{1}{\eta \langle : \hat{I}(t_1) : \rangle} \frac{\partial}{\partial t_1} \left[\sum_{k=1}^n P_k(t_1, t_2) \right]. \quad (2.30)$$

Recall the definition of the n th intensity correlation function, Eq. (2.6), and let us define once more $t_1 = t$ and $t_2 = t + \tau$. We want to remark that for times τ that are sufficiently small we can relate Eq. (2.21) and Eq. (2.22) to the n th order correlation function. The procedure is given as follows. Expanding the exponential in Eq. (2.23) we obtain the formulas for $P_n(t, t + \tau)$ and $w_n(\tau | t)$ in terms of correlations of the photon-flux operators at different times. At this point, we point out these formulas will prove extremely useful in the analysis of resonance fluorescence from a coherently driven two level atom. So, we write them out explicitly as

$$P_n(t, t + \tau) = \sum_{k=0}^{\infty} \frac{(k+n-1)! (-1)^k \eta^{n+k}}{(n-1)! k!} \int_0^{\tau} dt_{k+n-1} \int_0^{t_{k+n-1}} dt_{k+n-2} \dots \int_0^{t_2} dt_1 \times \\ \langle : \hat{I}(\tau + t) \hat{I}(t_{k+n-1} + t) \dots \hat{I}(t_1 + t) : \rangle, \quad (2.31)$$

$$w_n(\tau | t) = \frac{1}{\langle : \hat{I}(t) : \rangle} \sum_{k=0}^{\infty} \frac{(k+n-1)! (-1)^k \eta^{n+k}}{(n-1)! k!} \int_0^{\tau} dt_{k+n-1} \int_0^{t_{k+n-1}} dt_{k+n-2} \dots \int_0^{t_2} dt_1 \times \\ \langle : \hat{I}(\tau + t) \hat{I}(t_{k+n-1} + t) \dots \hat{I}(t_1 + t) \hat{I}(t) : \rangle. \quad (2.32)$$

Above we have used

$$\int_0^{\tau} dt_k \int_0^{\tau} dt_{k-1} \dots \int_0^{\tau} dt_1 \langle \mathcal{T} : \hat{I}(t_k + t) \dots \hat{I}(t_1 + t) : \rangle \\ = k! \int_0^{\tau} dt_k \int_0^{t_{k-1}} dt_{k-2} \dots \int_0^{t_2} dt_1 \langle : \hat{I}(t_k + t) \dots \hat{I}(t_1 + t) : \rangle \quad (2.33)$$

[8, 23]. When the detection efficiency is very small or wait time τ is very small, it is possible to truncate Eq. (2.31) and Eq. (2.32) up to an order of $\mathcal{O}(\eta^n)$. Doing so we obtain the

approximations [9]

$$\frac{P_n(t, t + \tau)}{\eta \langle : \hat{I}(t) : \rangle} \approx (\eta \langle : \hat{I}(t) : \rangle \tau)^{n-1} g^{(n)}(t, t), \quad (2.34)$$

$$\frac{w_n(\tau|t)}{\eta \langle : \hat{I}(t) : \rangle} \approx (\eta \langle : \hat{I}(t) : \rangle \tau)^{n-1} g^{(n+1)}(t, t). \quad (2.35)$$

It is well known that computing $g^{(n)}$ exactly for arbitrary n for any light field can be very difficult. Nonetheless, through the assumptions of small wait time τ or small efficiency of detection, we can get reasonable estimates of the n th order correlation function. First let us define the following ratio

$$g_n(t, t + \tau) = \lim_{n \ll 1} \frac{w_n(\tau|t)}{P_n(t, t + \tau)} \approx \frac{\langle : \hat{I}(t + \tau) [\hat{U}(t, t + \tau)]^{n-1} \hat{I}(t) : \rangle}{\langle : \hat{I}(t + \tau) [\hat{U}(t, t + \tau)]^{n-1} : \rangle \langle : \hat{I}(t) : \rangle} \quad (2.36)$$

From the form of $g_n(t, t + \tau)$, it is possible to approximate the n th coherence for a single value in time t , i.e. $g^{(n)}(t)$ for $n \geq 2$,

$$g^{(n)}(t) \approx \lim_{\tau \rightarrow 0} \left\{ \left[\prod_{j=1}^{n-1} g_j(t, t + \tau) \right] g^{(1)}(t, t + \tau) \right\}. \quad (2.37)$$

$g_n(t, t + \tau)$ is not a probability distribution and one may interpret it as follows. We now explain the meaning of g_n . For practical purposes let us invoke back the notation t_1 and t_2 . Also, recall the r -fold joint probabilities we have defined in Eq. (2.19) and consider the following enumerated conditions for small positive real numbers δt_1 and δt_2 (smaller than the coherence time of the photon sequence one considers):

1. $p^{(3)}(1, t_1 - \delta t_1, t_1; n - 1, t_1, t_2; 1, t_2, t_2 + \delta t_2)$ provides the joint probability that a photoelectric event is recorded in the interval $[t_1 - \delta t_1, t_1]$, followed by the occurrence of $n - 1$ photoelectric detection events, and a photoelectric detection recorded in the time interval $[t_2, t_2 + \delta t_2]$.
2. $p^{(3)}(0, t_1 - \delta t_1, t_1; n - 1, t_1, t_2; 1, t_2, t_2 + \delta t_2)$ is the joint probability that, regardless of whether or not a photoelectric detection is recorded at arbitrary time t_1 , $n - 1$ events must happen before the n th photoelectric detection event is recorded at time t_2 .

3. $p^{(1)}(1, t_1 - \delta t_1, t_1)$ is the probability that an event happened and was detected at time t_1 .
4. If it really is the case that a photoelectric detection recorded at time t_1 is related in any way on the occurrence of the following $n - 1$ photoelectric detections and the photoelectric detection at time t_2 then the joint probability in condition 1 is factorable in terms of the joint probabilities proportional to those in condition 2. and condition 3. If the photo electric detection recorded at time t_1 is strongly statistically related, and so are the following ones, then the probability in condition 1 is truly a non-factorable joint probability distribution of the $n + 1$ photoelectric detection events, meaning that recording the event at time t_2 is strongly conditional on the occurrence of previous photoelectric detection events.
5. When $p^{(1)}(1, t_1 - \delta t_1, t_1)$ is nonzero, and whenever $p^{(3)}(1, t_1 - \delta t_1, t_1; 0, t_1, t_2; 1, t_2, t_2 + \delta t_2)$ and $p^{(3)}(0, t_1 - \delta t_1, t_1; 0, t_1, t_2; 1, t_2, t_2 + \delta t_2)$ are zero but their ratio is not indeterminate, define the following ratio

$$\mathfrak{R} = \frac{p^{(3)}(1, t_1 - \delta t_1, t_1; n - 1, t_1, t_2; 1, t_2, t_2 + \delta t_2)}{p^{(3)}(0, t_1 - \delta t_1, t_1; n - 1, t_1, t_2; 1, t_2, t_2 + \delta t_2)p^{(1)}(1, t_1 - \delta t_1, t_1)}. \quad (2.38)$$

As $\delta t_1, \delta t_2 \rightarrow 0$ and $\eta \ll 1$, $\mathfrak{R} \rightarrow g_n(t, t + \tau)$.

6. If the first sentence of condition 4 is true, this would imply that $g_n(t, t + \tau) = 1$ for any photoelectric detection n . This tells us that events we are measuring are just completely random and uncorrelated. This is the case of coherent light and this implies $g^{(n)}(t, t + \tau) = 1$ which means a field has arbitrary degree of coherence [9].
7. If the second part of condition 4 is true then $g_n(t, t + \tau)$ is not necessarily 1 and thus possibly signaling a quantum property of the photoelectric detection sequence.

The above set of conditions do not serve as a formal proof for a physical interpretation of $g_n(t, t + \tau)$ but rather to illustrate an intuitive approach around a possible interpretation of

the ratio $g_n(t, t + \tau)$. Having acknowledged our thoughts, we now say that $g_n(t, t + \tau)$ could provide a measure of how “efficiently” or “deficient” a correlation of the n th photoelectric detection in a photon sequence is with respect to the first photoelectric detection at a given time t_1 . A possible valid advantage of g_n would be from the product formula in Eq. (2.37). That is, if the interval $[t, t + \tau]$ is to be partitioned, one could in principle get fragmented values for $g_j(j = 1, \dots, n)$ and thus estimate computationally a n th order coherence function.

Lastly, we point out that from Eq. (2.36), when $g_n(t, t + \tau) = 1$ and using the definition of \hat{U} from Eq.(2.13), we may have

$$\int_t^{t+\tau} dt_{n-1} \dots \int_t^{t+\tau} dt_1 [\langle : \hat{\mathcal{I}}(t_n, t_{n-1}, \dots, t_1, t) : \rangle - \langle : \hat{\mathcal{I}}(t_n, t_{n-1}, \dots, t_1) : \rangle \langle : \hat{I}(t) : \rangle] = 0, \quad (2.39)$$

where we have defined $\hat{\mathcal{I}}(t_n, t_{n-1}, \dots, t_1, t) = \hat{I}(t_n)\hat{I}(t_{n-1})\dots\hat{I}(t_1)\hat{I}(t)$ and $t_n = \tau$. Inspired by this and the definition of Mandel’s Q parameter we define

$$\begin{aligned} \mathcal{Q}_n(t, t+\tau) &= \int_t^{t+\tau} dt_{n-1} \dots \int_t^{t+\tau} dt_1 [\langle : \hat{\mathcal{I}}(t_n, t_{n-1}, \dots, t_1, t) : \rangle - \langle : \hat{\mathcal{I}}(t_n, t_{n-1}, \dots, t_1) : \rangle \langle : \hat{I}(t) : \rangle] \\ &= \int_t^{t+\tau} dt_{n-1} \dots \int_t^{t+\tau} dt_1 \langle : \hat{\mathcal{I}}(t_n, t_{n-1}, \dots, t_1) : \rangle \langle : \hat{I}(t) : \rangle \times \\ &\quad \left[\frac{\langle : \hat{\mathcal{I}}(t_n, t_{n-1}, \dots, t_1, t) : \rangle}{\langle : \hat{\mathcal{I}}(t_n, t_{n-1}, \dots, t_1) : \rangle \langle : \hat{I}(t) : \rangle} - 1 \right]. \end{aligned} \quad (2.40)$$

According to the interpretation of $g_n(t, t + \tau)$, we refer to $\mathcal{Q}_n(t, t + \tau) \neq 0$ as a measure of how much the statistics of the n th photodetection deviates from the n th photodetection from a random sequence of photons. We will not compute \mathcal{Q}_n for the specific light sources in this thesis but we instead remark that on defining $g_n(t, t + \tau)$ as we have defined in Eq. (2.36) gives rise to interesting notions on generalizations of Mandel’s Q parameter.

2.6 Unconditional and Conditional Average and Variance of Wait Time τ of the n th Photoelectric Detection

The average and variance of τ reveals us with the expected time ellapsed on average between photoelectric to photoelectric detections if the photon sequence is stationary [24]. Addition-

ally, the variance reveals to us the fluctuations of the wait time τ of these photoelectric detections. It may be of interest to study time averages of the unconditional and conditional wait time distributions since it is possible they could be potentially useful for calibration of delayed coincidences of photoelectric measurements.

In this section, we will assume for simplicity that the photon sequence we are dealing with is stationary. In this regime, the unconditional and conditional wait time distributions becomes $P_n(t, t + \tau) = P_n(\tau)$ and $w_n(\tau|t) = w_n(\tau)$. Using $t_1 = t$ and $t_2 = t + \tau$ and with the help of Eq. (2.26) and (2.14) and integration by parts, the mean and mean of the squared τ with respect of $P_n(\tau)$ can be expressed directly in terms of $G(s, \tau)$ as

$$\begin{aligned} \langle \tau \rangle_{P_n} &= \sum_{k=0}^{n-1} \frac{(-1)^k}{k!} \left[\frac{\partial^k}{\partial s^k} \int_0^\infty d\tau G(s, \tau) \right]_{s=1} = \frac{(-1)^{n-1}}{(n-1)!} \frac{\partial^{n-1}}{\partial s^{n-1}} \left[\frac{\int_0^\infty d\tau G(s, \tau)}{s} \right]_{s=1}, \quad (2.41) \\ \langle \tau^2 \rangle_{P_n} &= 2 \sum_{k=0}^{n-1} \frac{(-1)^k}{k!} \left[\frac{\partial^k}{\partial s^k} \int_0^\infty d\tau \tau G(s, \tau) \right]_{s=1} = 2 \frac{(-1)^{n-1}}{(n-1)!} \frac{\partial^{n-1}}{\partial s^{n-1}} \left[\frac{\int_0^\infty d\tau \tau G(s, \tau)}{s} \right]_{s=1}. \end{aligned} \quad (2.42)$$

Similarly, from Eqs. (2.28)-(2.30), the average and mean of the squared τ with respect of $w_n(\tau)$ will be given by

$$\langle \tau \rangle_{w_n} = \frac{1}{\eta \langle \hat{I} \rangle} \left(\sum_{k=1}^n \int_0^\infty d\tau P_k(\tau) \right) = \frac{n}{\eta \langle \hat{I} \rangle}, \quad (2.43)$$

$$\langle \tau^2 \rangle_{w_n} = \frac{2}{\eta \langle \hat{I} \rangle} \sum_{k=1}^n \int_0^\infty d\tau \tau P_k(\tau) = \frac{2}{\eta \langle \hat{I} \rangle} \sum_{k=1}^n \langle \tau \rangle_{P_k}. \quad (2.44)$$

Then the unconditional and conditional variance of wait time are respectively defined as

$$\langle (\Delta \tau)^2 \rangle_{P_n} \equiv \langle \tau^2 \rangle_{P_n} - \langle \tau \rangle_{P_n}^2 \quad (2.45)$$

$$\langle (\Delta \tau)^2 \rangle_{w_n} \equiv \langle \tau^2 \rangle_{w_n} - \langle \tau \rangle_{w_n}^2 = \frac{2}{\eta \langle \hat{I} \rangle} \sum_{k=1}^n \langle \tau \rangle_{P_k} - \frac{n^2}{(\eta \langle \hat{I} \rangle)^2}. \quad (2.46)$$

Chapter 3

Counting statistics of Coherent Light

Let us start our analysis by describing the properties of a photon sequence for coherent source of light. The photon sequence generated by a sufficiently coherent source can be regarded to be the output of a well-stabilized single-mode laser operating far above threshold. As we have mentioned, coherent light is characterized by a constant intensity photon sequence so that $\int_0^\tau \hat{I}(t)dt = \langle \hat{I} \rangle \tau$. For coherent light, it becomes evident that $g^{(n)}(t_1, \dots, t_k) = 1$ for arbitrary positive integers n and k and the Mandel's Q parameter satisfies $Q = 0$. Showing the Poissonian character of the statistics that describe coherent light. Using these remarks and Eqs.(2.12)-(2.14), the generating function and the photoelectric-count distribution for coherent light are found to be [5, 7]

$$G(s, \tau) = e^{-s\eta\langle \hat{I} \rangle \tau}, \quad (3.1)$$

$$p(n, \tau) = \frac{(\eta\langle \hat{I} \rangle \tau)^n e^{-\eta\langle \hat{I} \rangle \tau}}{n!}. \quad (3.2)$$

The generating function is thus a simple exponential and the photoelectric-count distribution is a Poisson distribution. This is expected since coherent light is described as a stationary constant rate Poisson point process. For such a random process, the successive events are uncorrelated. Consequently, the photoelectric measurements of coherent light initiated at a photo-detection (conditional) or initiated at random (unconditional) coincide. Hence, both the conditional and unconditional wait time distributions are given by

$$w_n(\tau) = \frac{\eta\langle \hat{I} \rangle (\eta\langle \hat{I} \rangle \tau)^{(n-1)}}{(n-1)!} e^{-\eta\langle \hat{I} \rangle \tau} = P_n(\tau). \quad (3.3)$$

In particular $P_1(\tau) = \eta\langle \hat{I} \rangle e^{-\eta\langle \hat{I} \rangle \tau} = w_1(\tau)$ are simple exponentials with $\tau = 0$ as the most probable wait time. Eq. (3.3) have the same functional form as that for a gamma distribution with shape parameter n and rate parameter $\eta\langle \hat{I} \rangle$ [25].

We can also calculate the mean and variance of wait time τ following the properties of the

gamma distribution. Notice also that it is not necessary to distinguish between unconditional and conditional averages since for coherent light both wait time distributions (conditional and unconditional) coincide. The mean and variance for the n th photoelectric detection in a coherent beam are given by

$$\langle \tau \rangle_n = \frac{n}{\eta \langle \hat{I} \rangle}, \quad (3.4)$$

$$\langle \Delta \tau^2 \rangle_n = \frac{n}{(\eta \langle \hat{I} \rangle)^2}. \quad (3.5)$$

The mean and the variance of τ sets a time scale we shall use for comparison of sub-Poissonian and super-Poissonian photon sequences as well as understanding bunched and anti-bunched photon sequences.

Chapter 4

Photon Counting Statistics of Thermal Light

Thermal light, also known as narrow-band Gaussian light, represents an ideal model for filtered light from electrical discharge lamps or the light from a single-mode laser cavity operating below threshold. In this chapter, we consider the source of thermal light to be a single-mode laser operating below threshold with mean cavity photon number \bar{n} , photon scape rate (cavity decay rate) 2γ and average photon-flux $\langle \hat{I} \rangle = 2\gamma\bar{n}$. The statistical description of the electric field amplitude for thermal light can be described by two real Gaussian variables with zero mean and equal variance or, equivalently, a single complex Gaussian random variable with mean zero and variance \bar{n} [26]. The generating function for a stationary thermal light beam obtained by the algorithm given in [27, 28] is

$$G(s, \tau) = \frac{e^{2\gamma\tau}}{\left[\cosh(z\tau) + \frac{1}{2} \left[\frac{z}{2\gamma} + \frac{2\gamma}{z} \right] \sinh(z\tau) \right]}. \quad (4.1)$$

Here $z^2 = (2\gamma)^2 + 2\eta(2\gamma)\langle \hat{I} \rangle s = (2\gamma)^2(1 + 2s\eta\bar{n})$. Using Eq. (2.14), one can find the photoelectric-count probability distribution is given recursively in terms of modified spherical Bessel functions [27], which can be used directly in Eqs. (2.26),(2.28) and (2.30) to obtain close expressions for $P_n(\tau)$ and $w_n(\tau)$. In general, the expressions obtained are intricate in their algebraic forms. Nevertheless, the forms for both $P_n(\tau)$ and $w_n(\tau)$ simplify noticeably for small and large mean photon number \bar{n} . Before we proceed to explain limiting case of the mean photon number, we provide useful expressions that will facilitate the calculations that lay ahead. Eq. (4.1) can be rewritten in more convenient form as

$$G(s, \tau) = [1 - A] \frac{e^{2\gamma\tau - z\tau}}{1 - Ae^{-2z\tau}}, \quad (4.2)$$

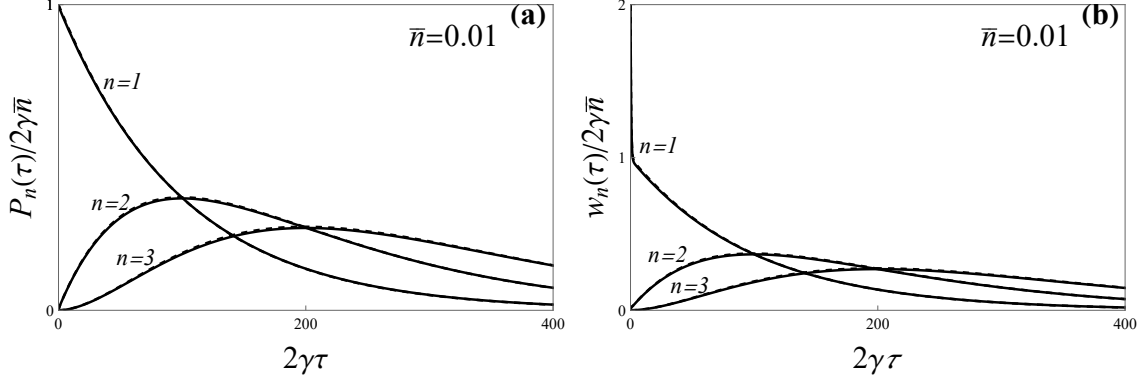


Figure 4.1: Comparison of the exact (solid black curves) and approximate (dashed black curves) expressions for $P_n(\tau)$ and $w_n(\tau)$ for $n = 1-3$ thermal photons for small $\bar{n} = 0.01$.

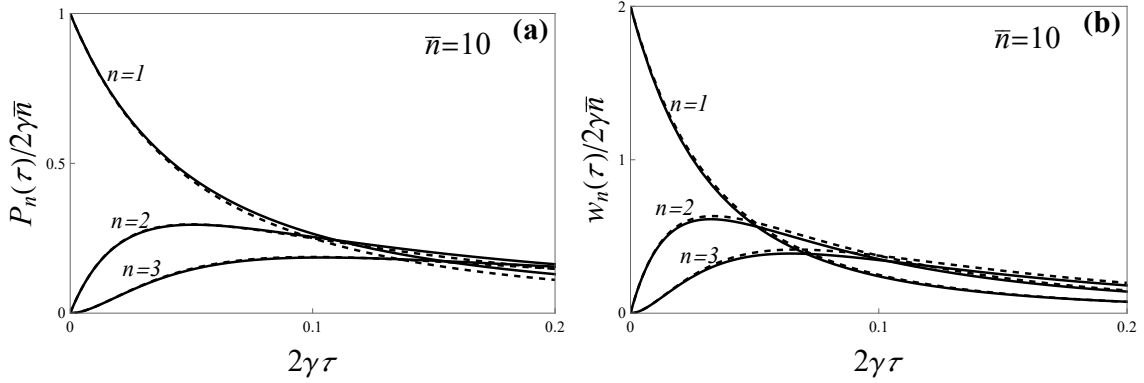


Figure 4.2: Comparison of the exact (solid black curves) and approximate (dashed black curves) expressions for $P_n(\tau)$ and $w_n(\tau)$ for $n = 1-3$ thermal photons for large $\bar{n} = 10$.

where

$$A = \left[\frac{z - 2\gamma}{z + 2\gamma} \right]^2. \quad (4.3)$$

The first two derivatives of the generating function $G(s, \tau)$ with respect to τ will also be given and they are given as

$$\frac{\partial}{\partial \tau} G(s, \tau) = G(s, \tau) \left[2\gamma - z - \frac{2Ae^{-2z\tau}}{1 - Ae^{-2z\tau}} \right], \quad (4.4)$$

$$\frac{\partial^2}{\partial \tau^2} G(s, \tau) = G(s, \tau) \left\{ \left[2\gamma - z - \frac{2Ae^{-2z\tau}}{1 - Ae^{-2z\tau}} \right]^2 + \frac{4z^2 Ae^{-2z\tau}}{1 - Ae^{-2z\tau}} + \frac{4z^2 A^2 e^{-4z\tau}}{(1 - Ae^{-2z\tau})^2} \right\}. \quad (4.5)$$

Using the above formulas, we now develop limiting cases for unconditional and conditional wait time distributions.

4.1 Small \bar{n} Limit

For the laser operating far below threshold, or equivalently, the laser cavity produces on average a very small number photons, $\bar{n} \ll 1$, we expect to see the distribution being dominated by long wait times. We expand Eq. (4.4) as power series of \bar{n} and take derivatives with respect to s and we keep as many terms necessary in order to satisfy the constraints imposed by Eqs. (2.34)-(2.35). As it turns out, the numbers of terms that need to be kept in the total approximate expressions for $P_n(\tau)$ is proportional to n , where n denotes the n th photoelectric detection. We then obtain the following expressions for the unconditional wait time distributions

$$P_1(\tau) \approx 2\eta\gamma\bar{n}e^{-2\eta\gamma\bar{n}\tau} \quad (4.6)$$

$$P_2(\tau) \approx 2\eta\gamma\bar{n}e^{-2\eta\gamma\bar{n}\tau} \frac{\eta\bar{n}}{2}(1 + 4\gamma\tau - e^{-4\gamma\tau}) \quad (4.7)$$

$$P_3(\tau) \approx 2\eta\gamma\bar{n}e^{-2\eta\gamma\bar{n}\tau} \frac{(\eta\bar{n})^2}{4}(1 + 8\gamma\tau + 8(\gamma\tau)^2 - e^{-4\gamma\tau}(12\gamma\tau + 1)). \quad (4.8)$$

A similar procedure using Eq. (4.5) for the conditional wait time distribution leads to

$$w_1(\tau) \approx 2\eta\gamma\bar{n}e^{-2\eta\gamma\bar{n}\tau}(1 + e^{-4\gamma\tau}) \quad (4.9)$$

$$w_2(\tau) \approx 2\eta\gamma\bar{n}e^{-2\eta\gamma\bar{n}\tau} \eta\bar{n}(1 + 2\gamma\tau + e^{-4\gamma\tau}(-1 + 6\gamma\tau)) \quad (4.10)$$

$$w_3(\tau) \approx 2\eta\gamma\bar{n}e^{-2\eta\gamma\bar{n}\tau} (\eta\bar{n})^2(1 + 3\gamma\tau + 3(\gamma\tau)^2 - e^{-4\gamma\tau}(2 + 3\gamma\tau - 18(\gamma\tau)^2) + e^{-8\gamma\tau}). \quad (4.11)$$

We compare Eqs. (4.6)- (4.11) in Fig. 4.2 with the exact expressions for both wait time distributions. The exact curves are given by using Eq. (4.1) in Eqs. (2.26) and (2.28). The solid curves represent exact expressions and the dashed curves represent the approximations. It can be seen that Eqs. (4.6)- (4.11) capture the essential properties of both wait time distribution for short and large wait times τ . For the $n = 1$ we can see that the normalized unconditional wait time distribution $P_1(\tau)/2\gamma\bar{n}$ is always 1 when $\tau = 0$ and it decreases monotonically for large τ . In the case of the normalized conditional wait time distribution

$w_1(\tau)/2\gamma\bar{n}$ it always starts with 2 when $\tau = 0$. More generally we further see

$$\lim_{n \ll 1} \frac{w_1(\tau)}{\eta \langle \hat{I} \rangle} = 1 + e^{-4\gamma\tau}. \quad (4.12)$$

that is $w_1(0)/2\gamma\eta\bar{n} = g^{(2)}(0)$ which for thermal light is known to have the value of 2 [2]. Unconditional and conditional wait time distributions for $2 \leq n$ start at 0 then reach a maximum value for some nonzero time τ which depends on n and then monotonically decay to zero as wait times become large. Furthermore, it is also remarkable that despite that statistical properties of thermal light have been thoroughly studied [5,27,28], the expressions given by Eqs. (4.6)- (4.11) have not appeared yet in the literature.

4.2 Large \bar{n} Limit

In the case $\bar{n} \gg 1$, the wait time distributions are expected to have a short time behavior, quickly decaying to zero for large wait times. Considering the limit $2\gamma\tau \ll 1$, the generating function given in Eq. (4.1) is approximated by [5, 19]

$$G(s, \tau) \approx \frac{1}{(1 + \eta s \bar{n} 2\gamma\tau)}. \quad (4.13)$$

Using the generating function above in Eqs. (2.14) we obtain the photoelectric-count probability

$$p(n, \tau) \approx \frac{(\eta\bar{n}2\gamma\tau)^n}{(1 + \eta\bar{n}2\gamma\tau)^{n+1}}. \quad (4.14)$$

We can now calculate the expression in square brackets from Eq. (2.26), before taking the derivative with respect to τ we have

$$\sum_{k=0}^{n-1} p(k, \tau) \approx 1 - \left[\frac{\eta\bar{n}2\gamma\tau}{1 + \eta\bar{n}2\gamma\tau} \right]^n. \quad (4.15)$$

An interesting feature of the above expression is that if we sum all the probabilities for all possible photon counts, i.e $n \rightarrow \infty$, we should get back unity, as it must be the case. Using

the above approximations Eq. (2.26) leads to unconditional wait time distribution

$$P_n(\tau) \approx 2\eta\gamma\bar{n} \frac{n(\eta\bar{n}2\gamma\tau)^{n-1}}{(1 + \eta\bar{n}2\gamma\tau)^{n+1}}. \quad (4.16)$$

In a similar fashion we have that the expression in square brackets from (2.28) evaluates to

$$\sum_{k=0}^{n-1} (n-k)p(k, \tau) \approx n - \eta\bar{n}2\gamma\tau \left\{ 1 - \left[\frac{\eta\bar{n}2\gamma\tau}{1 + \eta\bar{n}2\gamma\tau} \right]^n \right\} \quad (4.17)$$

and taking then the derivatives derivatives with respect to τ as given by Eq. (2.28) gives the conditional wait time distribution

$$w_n(\tau) \approx 2\eta\gamma\bar{n} \frac{n(n+1)(\eta\bar{n}2\gamma\tau)^{n-1}}{(1 + \eta\bar{n}2\gamma\tau)^{n+2}}. \quad (4.18)$$

Eqs. (4.14)-(4.18) are illustrated in Fig. 4.2 and compared with exact expressions. The approximations can be seen to have excellent agreement with the exact wait time distributions for short wait time. The above equation also satisfy the impositions given by Eqs. (2.34)-(2.35).

Consider now the long time behavior. For long times $1 \ll 2\gamma\tau$ the generating function for thermal light is given by [29]

$$G(s, \tau) \approx \frac{4(1 + 2s\eta\bar{n})^{1/2}}{[1 + (1 + 2s\eta\bar{n})^{1/2}]^2} e^{-2\gamma\tau((1+2s\eta\bar{n})^{1/2}-1)}. \quad (4.19)$$

The expression above gives an exponential tail distribution when $\bar{n} \ll 1$ characteristic of coherent light. Furthermore, in the long time limit we can further simplify the generating function by realizing that in this long time regime the integrated photon-flux $\hat{U}(\tau) = \int_0^\tau \hat{I}(t)dt \approx \langle \hat{I} \rangle \tau = 2\gamma\tau\bar{n}$. We further simplify and have

$$G(s, \tau) = e^{-2s\eta\bar{n}\tau} - \mathcal{O}((s\bar{n})^2). \quad (4.20)$$

the generating function given in the equation above has the same form of the generating function of that of coherent light. It is then expected that the long time behavior of thermal light is coherent with photon rate $2\eta\gamma\bar{n}$. We further notice that Eqs. (4.6)- (4.11) for wait

time distributions have the expected exponential tail $e^{-2\gamma\eta\tau}$. The expressions given by Eqs. (4.16)-(4.18) do not have this exponential tail since they predict a slower fall off for small wait times ($2\gamma\tau \ll 1$), nevertheless, they capture quite remarkably well the behavior of the exact expressions as \bar{n} increases. The large \bar{n} limit is known as the high degeneracy- large mode occupation number-limit.

From Eqs. (4.16)-(4.18) we see that for thermal light the unconditional and conditional wait time distributions are related by the functional relation

$$w_n(\tau) \approx \frac{(n+1)}{(1+\eta\bar{n}2\gamma\tau)} P_n(\tau) \quad (4.21)$$

Additionally, $P_2(\tau)$ and $w_1(\tau)$ are proportional to the second order intensity coherence function $g^{(2)}(0)$ for short times, as both distributions involve the detection of a pair of photons. In the case of the unconditional wait time distribution, $P_2(0) = 0$. This implies that if counting process commences at arbitrary instant, the second photo-detection occur after a wait time τ , and it must be the case that a photo detection have already occurred. On the other hand, the normalized wait time distribution for the *first* photoelectric detection is 2 (which is the maximum value of $w_1(\tau)/2\gamma\bar{n}$). This tells us that if one starts the counting process at a detection of a photon, the photo-detection after counting began is most likely to occur immediately after counting starts. In other words, thermal photons are bunched temporally- the detection of a photon makes the detection of another photon short after highly probable.

We further explore the bunching property of thermal light by pointing out few remarks on the n th order coherence. Note that in both cases of the small and large mean photon number it can be shown that Eq. (2.36), by using our approximations, satisfies $g_n(0) = (n+1)$. Therefore using Eq. (2.37), we have $g^{(n)}(0) = n!$ which is a result well known for chaotic Gaussian light [4]. It is also interesting to notice that in the large mean photon number limit

$$g_n(\tau) \approx \frac{(n+1)}{(1+\eta\bar{n}2\gamma\tau)}, \quad (4.22)$$

and thus $g_n(0) > g_n(\tau)$.

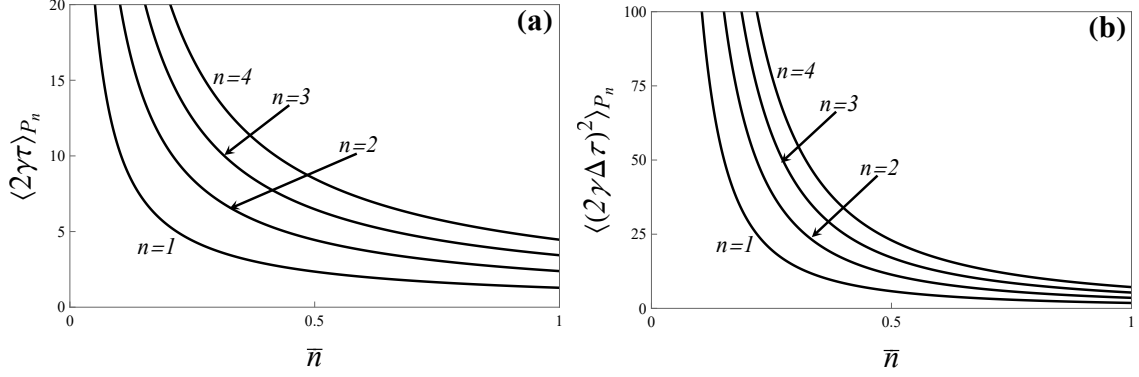


Figure 4.3: Unconditional average and variance of wait time τ for the photodetections $n = 1 - 4$. We do not include averages and variances with respect to w_n since the are given in terms of the averages and variances with respect to P_n .

Lastly, the average unconditional and conditional wait time and its variance for thermal photons can be computed using Eqs. (2.41)-(2.42). Analytic expressions in terms of hypergeometric functions can be obtained. The resulting averages of τ and τ^2 are expressions that are not very illuminating but for completeness they are given by

$$\langle \tau \rangle_{P_n} = \frac{1}{\gamma} \sum_{k=0}^{n-1} \frac{(-1)^k}{k!} \frac{d^k}{ds^k} \left[\left(\frac{z}{2\gamma} + 1 \right)^{-2} \Phi \left(\frac{(z-2\gamma)^2}{(z+2\gamma)^2}, 1, \frac{1}{2} \left(1 - \frac{2\gamma}{z} \right) \right) \right] \Big|_{s=1}, \quad (4.23)$$

$$\langle \tau^2 \rangle_{w_n} = \frac{1}{\eta \bar{n} \gamma^2} \sum_{k=0}^{n-1} \frac{(-1)^k (n-k)}{k!} \frac{d^k}{ds^k} \left[\left(\frac{z}{2\gamma} + 1 \right)^{-2} \Phi \left(\frac{(z-2\gamma)^2}{(z+2\gamma)^2}, 1, \frac{1}{2} \left(1 - \frac{2\gamma}{z} \right) \right) \right] \Big|_{s=1}, \quad (4.24)$$

and

$$\langle \tau^2 \rangle_{P_n} = \frac{1}{2\gamma^2} \sum_{k=0}^{n-1} \frac{(-1)^k}{k!} \frac{d^k}{ds^k} \left[\left(\frac{z}{2\gamma} \right)^{-1} \left(\frac{z}{2\gamma} + 1 \right)^{-2} \Phi \left(\frac{(z-2\gamma)^2}{(z+2\gamma)^2}, 2, \frac{1}{2} \left(1 - \frac{2\gamma}{z} \right) \right) \right] \Big|_{s=1}, \quad (4.25)$$

where $\Phi(z, s, a)$ are the Lerch's Transcendent functions [37].

It can be seen from Fig. 4.3 that both the mean and variance decrease to zero monotonically for all n as \bar{n} increases. On the other hand, in the small mean photon number regime we can approximate the equation above. Therefore the leading term for conditional and unconditional averages and variances of wait time τ are given the leading term in \bar{n} as

$$\langle \tau \rangle_{P_n} = \frac{n}{\eta \bar{n} 2\gamma}. \quad (4.26)$$

In the same limit, the average of the square wait time τ with respect to unconditional and conditional wait time distribution has leading order given by

$$\langle \tau^2 \rangle_{P_n} = \frac{n(n+1)}{(\eta \bar{n} 2\gamma)^2} = \langle \tau^2 \rangle_{w_n}. \quad (4.27)$$

The leading terms on variance of wait times comes to be equal to that of coherent light with the average photon flux $2\eta\gamma\bar{n}$. This is expected since for very small \bar{n} the laser is operating far below threshold and the photoelectric detections we expect to record are rather rare. Then, we may be interpret these photoelectric recordings as random events.

Consider the most probable times for coherent light. These are easily obtained from Eq. (3.3). We thus have that for thermal light the most probable time is $\tau_{n,coh} = (n - 1)/\eta\langle\hat{I}\rangle$, where $\langle\hat{I}\rangle$ again is the average photon flux. We now consider the large mean photon number limit. Based on Eq. (4.16), the most probable wait times for the unconditional n th photodetection is given to be $\tau_{n,th} = (n - 1)/2\eta\langle\hat{I}\rangle$, which is shorter than $\tau_{n,coh}^P$. From Eq. (4.18), the most probable time is $\tau_{n,coh}^w = (n - 1)/3\eta\langle\hat{I}\rangle$, which is even shorter than $\tau_{n,coh}^P$. The most probable times for thermal light are shorter that that for coherent light since thermal light is bunched. Refer to Figure 4.3 for the plots of the unconditional variances.

Chapter 5

Photon Counting Statistics of the Degenerate Parametric Oscillator

5.1 Description of the DPO

The degenerate parametric oscillator (DPO) is one of the most important sources of squeezed light. It requires a fully quantum mechanical treatment to completely describe its statistical properties. The basic mechanism of the DPO is the conversion of a pump photon into a pair of photons in a sub-harmonic mode (down-conversion) of an optical cavity. The process occurs in a nonlinear medium where photon energy and momentum are conserved. The Hamiltonian describing the above process is given as

$$\hat{H} = \frac{1}{2}i\hbar(\kappa\hat{a}_d^{\dagger 2}\hat{b} - \kappa^*\hat{a}_d^2\hat{b}^\dagger) + i\hbar\Gamma(\epsilon\hat{b}^\dagger - \epsilon^*\hat{b}) + \hat{H}_{Loss}. \quad (5.1)$$

Where κ is the mode coupling constant given by the third order susceptibility of the nonlinear medium, \hat{b}, \hat{b}^\dagger are the annihilation and creation operators for the photons in the pump mode, \hat{a}, \hat{a}^\dagger , are the annihilation and creation for the photons in the sub-harmonic mode, ϵ is a dimensionless classical field amplitude which is defined such that $|\epsilon|^2$ is the number of photons incident on the cavity in one lifetime $(2\Gamma)^{-1}$ at the pump mode. \hat{H}_{Loss} describes losses of the cavity [30]. An equation of motion for the density matrix can be derived from the above Hamiltonian when using the Markov approximation in the Heisenberg equation of motion or master equation [10, 15]. It is required to use an appropriate quasi-probability distribution since the coherent state diagonal representation leads to complications on the Fokker-Planck equation for probability distribution describing the process. Using the positive- \mathcal{P} representation [11] one can derive a Fokker-Planck equation with positive diffusion. Two Langevin equations can be derived for the sub-harmonic mode without the effects of pump depletion.

Their expressions are given by [15, 31, 32]

$$\dot{\alpha} = -\gamma\alpha + \kappa\epsilon\alpha_* + \sqrt{\kappa\epsilon}\xi_1(t), \quad (5.2)$$

$$\dot{\alpha}_* = -\gamma\alpha_* + \kappa\epsilon\alpha + \sqrt{\kappa\epsilon}\xi_2(t). \quad (5.3)$$

Each variable α and α_* corresponds to the creation and annihilation operators of the sub-harmonic mode and they are not complex conjugate of each other. Each ξ_1 and ξ_2 are Gaussian white-noise stochastic processes with mean zero and variance equals to 1. Above, sub-harmonic photons escape from the cavity at rate 2γ and photon-flux $I(t) = 2\gamma\alpha\alpha_*$. By setting $\kappa\epsilon = |\kappa\epsilon|e^{i\varphi}$, $\alpha = xe^{i\varphi/2}$ and $\alpha_* = xe^{-i\varphi/2}$, for an arbitrary real number φ , one obtains the equivalent equations of motion for the newly defined variables x and y . Setting the initial state of the oscillator to the vacuum state with $x = 0 = y$ ensures that the new variables x and y remain real in time. To uncouple the equations of motion of x and y we define

$$u_i = \frac{x \pm y}{2}, \quad \lambda_i = \gamma \mp |\kappa\epsilon|, \quad q_i(t) = \frac{\xi_1 \pm \xi_2}{2}. \quad (5.4)$$

with $i = \{1, 2\}$. These transformations lead to the following equation of motion for u_i

$$\dot{u}_i(t) = -\lambda_i u_i(t) + \sqrt{\frac{|\kappa\epsilon|}{2}} q_i(t), \quad (5.5)$$

with steady state solutions

$$u_i(t) = \sqrt{\frac{|\kappa\epsilon|}{2}} \int_{-\infty}^t e^{-\lambda_i(t-t')} q_i(t') dt'. \quad (5.6)$$

Since q_i 's are defined by linear combinations of ξ_1 and ξ_2 , they are also Gaussian white-noise processes and satisfy

$$\langle q_i(t) \rangle = 0, \quad \langle q_i(t) q_j(t') \rangle = \delta_{ij} \delta(t - t'). \quad (5.7)$$

Using the equations above and Eq. (5.6) we obtain the mean and variance for the variables u_i

$$\begin{aligned}\langle u_i(t) \rangle &= 0, \\ \langle u_i(t)u_j(t') \rangle &= \frac{|\kappa\epsilon|}{4\lambda_i} \delta_{ij} e^{-\lambda_i|t'-t|}.\end{aligned}\tag{5.8}$$

The photon count statistics and unconditional and conditional wait distributions P_1 and w_1 for squeezed light from a DPO are fully described in [30]. We only introduced the variables α , α_* , u_1 , and u_2 briefly since they are of vital importance in understanding the DPO. We also define the mean photon number of squeezed light from a DPO as \bar{n} and is given by

$$\bar{n} = \frac{1}{2} \left[\frac{|\kappa\epsilon|^2}{\gamma^2 - |\kappa\epsilon|^2} \right].\tag{5.9}$$

Consider now the generating function $G(s, T)$ for squeezed light produced by a DPO operating below threshold. The exact expression is then found to have the form $G(s, \tau) = Q_1(s, \tau)Q_2(s, \tau)$, with $Q_i(s, \tau)$ given by [30, 33]:

$$Q_i(s, \tau) = \frac{e^{\lambda_i\tau/2}}{\left[\cosh(z_i\tau) + \frac{1}{2} \left[\frac{z_i}{\lambda_i} + \frac{\lambda_i}{z_i} \right] \sinh(z_i\tau) \right]^{\frac{1}{2}}},\tag{5.10}$$

where $z_i^2 = \lambda_i^2 \pm 2s\eta\gamma\kappa\epsilon$ for $i = \{1, 2\}$. It is interesting to note that the statistics of the thermal light is described by two real Gaussian random process with zero mean but both with the same variance which is equivalent to a single Gaussian stochastic process [26]. This gives rise to the expression for the generating function for thermal light given by Eq. (4.1). In the case of squeezed light from a DPO, we have the same variables as thermal light but they now have different variance. This difference spurs particular and very distinct quantum statistical properties for both thermal and DPO light.

Consider first the unit detection efficiency $\eta = 1$. When we use Eq. (5.10) in Eqs. (2.14), (2.26), and (2.28) the expressions resulting for the unconditional and conditional wait time distributions $P_n(\tau)$ and $w_n(\tau)$ cannot be represented in terms of elementary functions. The resulting expressions are rather convoluted and complicated and thus will not be reproduced

here. However, there exists important limiting cases such as small and large mean photon number \bar{n} and wait time τ for which we obtain reasonable analytic expressions which are given in terms of very simple algebraic functions, and which are consistent with the exact results in their respective domain of approximation. The limiting cases are discussed in the following sections.

5.2 Small Mean Cavity Photon Number \bar{n}

Consider the case of small mean cavity photon number ($\bar{n} \ll 1$) and, therefore, small photon-flux. In this case, the wait times will be dominated by large intervals $2\gamma\tau \gg 1$. In this limit, the generating function and the photo-count distribution take the form [30, 33, 34]

$$G(s, \tau) \approx \left[1 - \frac{\bar{n}}{2}s^2\right] \exp[\gamma\bar{n}\tau(s^2 - 2s)] , \quad (5.11)$$

$$p(2k, \tau) \approx \frac{(\bar{n}\gamma\tau)^k}{k!} e^{-\bar{n}\gamma\tau} , \quad (5.12)$$

$$p(2k + 1, \tau) \approx \bar{n} \frac{(\bar{n}\gamma\tau)^k}{k!} e^{-\bar{n}\gamma\tau} . \quad (5.13)$$

An inspection of Eqs. (5.12) and (5.13) reveals a peculiar nature of the photo-count distribution of the photon sequence generate by a DPO. We find that the probability of detecting an odd number of photo-counts is negligible compared to the probability of detecting an even number of photo-counts ($p_{2k+1}/p_{2k} \approx \bar{n} \ll 1$). It's as if the cavity favors the emission of pairs of photons. This picture is reinforced by the structure of Eq. (5.12). Note that a mean photo-emission rate $2\gamma\bar{n}$ will result in $2\gamma\bar{n}\tau$ photon counts (corresponding to $\bar{n}\gamma T$ photon-pairs) in time τ . Eq. (5.12) then shows that the probability of recording $2k$ photo-counts is the same as the probability of recording k (random) photon-pairs. To understand the significance of this result let us recall that the nonlinear interaction between the pump and cavity modes in the DPO creates photon pairs inside the cavity. Once inside the cavity, each photon from each photon pair created in the sub-harmonic mode circulates, not necessarily following the same path but independently, escaping the cavity in a life time $(2\gamma)^{-1}$. Based on this pic-

ture, we do not expect a pair-like photo-count distribution Eqs. (5.12)-(5.13) even though the photons are created in pairs. However, for sufficiently low \bar{n} , the rate of photon-pair generation in the cavity is small, such that both photons of a pair escape the cavity before another pair is created. Thus a detector monitoring the output will still record, with high probability, an even number of photon counts in a time τ large compared with the cavity life time $(2\gamma)^{-1}$. The mean cavity photon number ($\bar{n} \ll 1$) and the mean photon flux $2\gamma\bar{n}$ (compared to 2γ) remain small.

Given that photon-count probabilities favor even photon counts over odd photon counts, we thus see the same behavior reflected in the unconditional and conditional wait time distributions $P_n(\tau)$ and $w_n(\tau)$. If we are to use Eqs. (5.11),(5.12) and (5.13) in Eqs. (2.26) and (2.28) long wait time behavior can be well approximated. However, the resulting expressions will not capture the short time behavior. We will have to expand the generating function and its derivatives with respect to τ for the DPO, Eq. (5.10), to include higher orders of \bar{n} constrained by Eqs. (2.34) and (2.35) to correctly capture the short time behavior of the wait time distributions as it was the case for thermal light.

In similar fashion as we have done for thermal light, we rewrite the generating function for the light from a DPO in a more convenient form [30] as

$$G(s, \tau) = [(1 - A_1)(1 - A_2)]^{1/2} \frac{e^{(2\gamma - z_1 - z_2)\tau/2}}{[(1 - A_1 e^{-2z_1\tau})(1 - A_2 e^{-2z_2\tau})]^{1/2}}, \quad (5.14)$$

where

$$A_1 = \left[\frac{z_1 - \lambda_1}{z_1 + \lambda_1} \right]^2, \quad (5.15)$$

$$A_2 = \left[\frac{z_2 - \lambda_2}{z_2 + \lambda_2} \right]^2. \quad (5.16)$$

The first two derivatives of $G(s, \tau)$ with respect to wait time τ are given as

$$\frac{\partial}{\partial \tau} G(s, \tau) = G(s, \tau) \left[\frac{1}{2}(2\gamma - z_1 - z_2) - \frac{z_1 A_1 e^{-2z_1\tau}}{1 - A_1 e^{-2z_1\tau}} - \frac{z_2 A_2 e^{-2z_2\tau}}{1 - A_2 e^{-2z_2\tau}} \right], \quad (5.17)$$

$$\frac{\partial^2}{\partial \tau^2} G(s, \tau) = G(s, \tau) \left\{ \left[\frac{1}{2}(2\gamma - z_1 - z_2) - \frac{z_1 A_1 e^{-2z_1 \tau}}{1 - A_1 e^{-2z_1 \tau}} - \frac{z_2 A_2 e^{-2z_2 \tau}}{1 - A_2 e^{-2z_2 \tau}} \right]^2 + \frac{2z_1^2 A_1^2 e^{-2z_1 \tau}}{(1 - A_1 e^{-2z_1 \tau})^2} + \frac{2z_2^2 A_2^2 e^{-2z_2 \tau}}{(1 - A_2 e^{-2z_2 \tau})^2} \right\}. \quad (5.18)$$

Expanding the above formulas in powers of \bar{n} and taking appropriately derivatives with respect to s can correctly provide the short and long time scales of the wait time distributions.

This leads us to the unconditional wait time distribution for $n = 1 - 3$ photo-detections

$$P_1(\tau) \approx 2\gamma\bar{n}e^{-\gamma\bar{n}\tau}(1 + e^{-2\gamma\tau}), \quad (5.19)$$

$$P_2(\tau) \approx 2\gamma\bar{n}e^{-\gamma\bar{n}\tau}\frac{1}{2}(1 - e^{-2\gamma\tau}), \quad (5.20)$$

$$P_3(\tau) \approx 2\gamma\bar{n}e^{-\gamma\bar{n}\tau}\frac{\bar{n}}{2}(3 + \gamma\tau + 3e^{-4\gamma\tau} - e^{-2\gamma\tau}(6 + \gamma\tau - 4(\gamma\tau)^2)). \quad (5.21)$$

The exact algorithm leads the following expressions for the conditional wait time distribution

$$w_1(\tau) \approx 2\gamma\bar{n}e^{-\gamma\bar{n}\tau} \left[\frac{1}{4} + e^{-4\gamma\tau} + e^{-2\gamma\tau} \left(\frac{1}{2\bar{n}} + \frac{7}{4} \right) \right], \quad (5.22)$$

$$w_2(\tau) \approx 2\gamma\bar{n}e^{-\gamma\bar{n}\tau} \left[\frac{1}{2} - 2e^{-4\gamma\tau} + e^{-2\gamma\tau} \left(\frac{3}{2} + 4\gamma\tau \right) \right], \quad (5.23)$$

$$w_3(\tau) \approx 2\gamma\bar{n}e^{-\gamma\bar{n}\tau} \left[\frac{1}{4} + e^{-4\gamma\tau} + e^{-2\gamma\tau} \left(2(\gamma\tau)^2 + \frac{3}{2}\gamma\tau - \frac{5}{4} \right) \right]. \quad (5.24)$$

Eqs. (5.19)-(5.24) are plotted and compared with the exact distributions in Figs. 5.1 and 5.2. The dashed curves are given by the approximations and the solid curves are given by the exact expressions. Notice that approximations capture the short and large wait time behavior of the wait time distributions.

Let us point out properties that become apparent from Eqs. (5.19)-(5.24). First of all, similar to the wait time distributions for thermal light, P_1 and w_1 are not zero at $\tau = 0$ and as τ increases both distributions decay exponentially to zero. It is also notable that in the short time regime the conditional wait time distribution w_1 reveals that a photon sequence from a DPO is “super-thermal.” This can be seen from the short wait time approximation that $w_1(\tau) \propto \langle : \hat{I}(0)^2 : \rangle$, which for DPO is $\propto \bar{n}^2$ and for thermal light is $\propto \bar{n}$. Since $\bar{n} \ll 1$, then $\bar{n}^2 \ll \bar{n}$ [5,30,34], we then have that $g_{th}^{(2)}(0) < g_{dpo}^{(2)}(0)$. For $n \leq 2$, the distributions reach

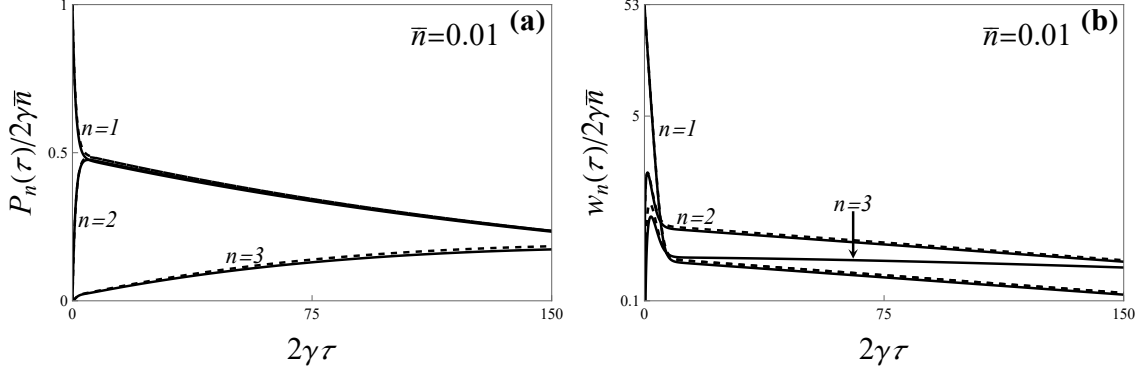


Figure 5.1: Exact curves (solid black) and approximations (dashed black curves) for $P_n(\tau)$ and $w_n(\tau)$ for the case that $\bar{n} \ll 1$ for DPO $n = 1-3$ photons.

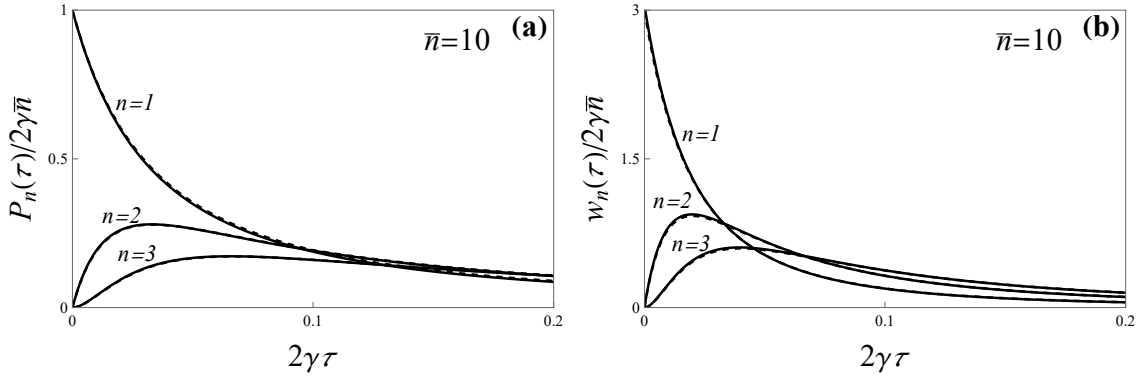


Figure 5.2: Exact curves for $P_n(\tau)$ and $w_n(\tau)$ for squeezed light from a DPO for $n = 1-3$ compared with approximate expressions (dashed curves) given by Eqs. (5.28) and (5.30) for $\bar{n} = 10$.

a maximum at wait time τ and then decay exponentially to zero. Secondly, Eqs. (5.19)-(5.24) are described by two distinct time scales, the short time scale $(2\gamma)^{-1}$ and the long time scale $(\gamma\bar{n})^{-1}$. The short time scale $(2\gamma)^{-1}$ is the inverse of photo-emission rate when the cavity has one photon. This photo-emission rate far exceeds the average photo-emission rate $(\gamma\bar{n})^{-1}$. It can be thought of as photo-emission rate conditioned on a photo-detection. In the small \bar{n} regime, the cavity has either a pair of photons (for a period lasting one cavity life time) or no photons. The detection of a photon in this regime signals, with high probability, the presence of one photon in the cavity, resulting in a photo-emission rate 2γ following a photodetection. This is a manifestation of strong nonclassical correlations between the photons of a photon-pair produced in the process of downconversion. The long time scale $(\gamma\bar{n})^{-1}$ is the inverse of

photon pair emission rate. Indeed, the long wait time tail of these distributions is Poissonian with mean flux $\gamma\bar{n}$, which is half the mean photon flux $2\gamma\bar{n}$ from the cavity. Also, for large wait times $2\gamma\tau \gg 1$, $P_1 \approx P_2$ and $P_3 \approx P_4$. The pattern, in fact, extends to higher order distributions with $P_{2k+1} \approx P_{2k+2}$. Thus the long wait time behavior mimics a random photon sequence of mean flux $\gamma\bar{n}$ and not $2\gamma\bar{n}$. Both of these aspects reflect the pair-like character of photo-emissions from the DPO in the small mean cavity photon number \bar{n} regime.

5.3 Large Mean Photon Number $\bar{n} \gg 1$

The large photon number regime is also of practical interest. As the oscillator approaches threshold of oscillation, many photon pairs are created inside the cavity in a cavity life time and the photons escaping the DPO cavity cannot be interpreted as coming from the same pair [30]. In this case, the wait times are dominated by intervals small compared to the cavity lifetime $(2\gamma)^{-1}$ and the generating function $G(s, \tau)$ can be approximated by [30, 33]

$$G(s, \tau) \approx \frac{1}{\sqrt{1 + 4s\eta\gamma\bar{n}\tau}} \quad (5.25)$$

Using Eq. (2.14) we obtain an analytic expression for the photoelectric count probability $p(n, t)$

$$p(n, \tau) \approx \frac{(2n-1)!!}{n!} \frac{(2\eta\gamma\bar{n}\tau)^n}{(1 + 4\eta\gamma\bar{n}\tau)^{n+1/2}}. \quad (5.26)$$

Once more, one calculates the expression in square brackets from Eq. (2.26), before the derivative with respect to τ and using the definitions of Hyper-geometric functions [35] one obtains

$$\sum_{k=0}^{n-1} p(k, \tau) \approx 1 - \frac{(2\eta\gamma\bar{n}\tau)^{n-1}}{(1 + 4\eta\gamma\bar{n}\tau)^{n-1/2}} \frac{(2n-1)!!}{n!} {}_2F_1 \left[\begin{matrix} 1, n + \frac{1}{2} \\ n + 1 \end{matrix}; 2 \frac{2\eta\gamma\bar{n}\tau}{1 + 4\eta\gamma\bar{n}\tau} \right]. \quad (5.27)$$

As a check, the limit $n \rightarrow \infty$ also gives 1 for the above expression. Taking the derivative with respect to τ as given by Eq. (2.26) leads to

$$P_n(\tau) \approx 2\eta\gamma\bar{n} \frac{(2n-1)!!}{(n-1)!} \frac{(2\eta\gamma\bar{n}\tau)^{n-1}}{(1+4\eta\gamma\bar{n}\tau)^{n+1/2}}. \quad (5.28)$$

In a similar fashion we have

$$\begin{aligned} \sum_{k=0}^{n-1} (n-k)p(k, \tau) &\approx n - \eta\bar{n}2\gamma\tau \\ &+ \frac{(2\eta\gamma\bar{n}\tau)^n}{(1+4\eta\gamma\bar{n}\tau)^{n+1/2}} \frac{(2n-1)!!}{(n-1)!} \left\{ {}_2F_1 \left[\begin{matrix} 1, n + \frac{1}{2} \\ n \end{matrix}; 2 \frac{2\eta\gamma\bar{n}\tau}{1+4\eta\gamma\bar{n}\tau} \right] - {}_2F_1 \left[\begin{matrix} 1, n + \frac{1}{2} \\ n+1 \end{matrix}; 2 \frac{2\eta\gamma\bar{n}\tau}{1+4\eta\gamma\bar{n}\tau} \right] \right\}. \end{aligned} \quad (5.29)$$

Taking then the derivatives as described in Eq. (2.28) gives

$$w_n(\tau) = 2\eta\gamma\bar{n} \frac{(2n+1)!!}{(n-1)!} \frac{(2\eta\gamma\bar{n}\tau)^{n-1}}{(1+4\eta\gamma\bar{n}\tau)^{n+3/2}}. \quad (5.30)$$

A comparison of Eqs. (5.28) and (5.30) are given in Fig. 5.2, and one can see that there is a good agreement for short wait times with the exact distributions. Similar to the case of thermal light, when we compare the expressions for the large mean photon number against those approximations for the small mean photon numbers, the two time scales $(2\gamma)^{-1}$ and $(\bar{n}\gamma)^{-1}$ are replaced by a single time scale $(2\eta\bar{n}\gamma)^{-1}$ determined by the mean photon flux of the cavity, $2\gamma\bar{n}$ and quantum efficiency of the detector. This limit is also known as the high degeneracy limit of squeezed light thoroughly discuss in Ref. [19].

Once more, the unconditional and conditional wait time distributions are related by

$$w_n(\tau) = \frac{(2n+1)}{1+4\eta\gamma\bar{n}\tau} P_n(\tau), \quad (5.31)$$

which is remarkably similar to the expression given by Eq. (4.21) for thermal light. There are other similarities, for example. The approximations for the large mean photon number shown in Fig. 4.2 and Fig. 5.2 demonstrate that both set of approximation, for thermal light and DPO, are qualitatively similar. Also the most probable conditioned wait times for DPO are

given by $\tau_{n,dpo}^w = (n-1)/5\langle\hat{I}\rangle$. And compared to the thermal case, $\tau_{n,th}^w = (n-1)/3\langle\hat{I}\rangle$, we see that the most probable conditional wait time for DPO is even shorter than the most probable time for thermal light. Lastly, consider Eqs. (2.36) and (2.37). We see that $g_n(0) = (2n+1)$. This then implies that $g^{(n)}(0) = (2n-1)!!$ which is a characteristic property of squeezed light [1].

To finalize our discussion on wait times statistics for squeezed light from a DPO, we discuss the mean and variance of the unconditional and conditional wait times τ for the DPO. In the general sense, Eqs. (2.41)-(2.46) can be solved exactly and it is shown that the exact expressions are given in terms of Hyper-geometric functions of higher order. However, other than being a formidable algebraic task there is not much one could extract by looking at these expressions. For continuity however, we only consider the expressions for mean and variance with respect to both unconditional and conditional wait time distributions when there is small mean photon number, $\bar{n} \ll 1$.

To start our derivation, we can use a similar procedure as the one used to derive Holder's inequality or Schwartz inequality for integrals [35,36] to show that we can write for two real valued distributions $0 \leq q_1(s, \tau), q_2(s, \tau)$:

$$\int_0^\infty q_1(s, \tau)q_2(s, \tau)d\tau = [(1 - A_1)(1 - A_2)]^{1/2} \left[\int_0^\infty q_1^2(s, \tau)d\tau \int_0^\infty q_2^2(s, \tau)d\tau \right]^{1/2} (1 - e)^{1/2} \quad (5.32)$$

where

$$q_i(s, \tau) = \frac{e^{(2\gamma - z_1 - z_2)\tau/4}}{[1 - A_i e^{-2z_i\tau}]^{1/2}},$$

$$e = \frac{\int_0^\infty \int_0^\infty [q_1(s, x)q_2(y) - q_2(s, x)q_1(s, y)]^2 dx dy}{2\sqrt{\int_0^\infty q_1^2(s, \tau)d\tau \int_0^\infty q_2^2(s, \tau)d\tau}} \quad (5.33)$$

In the above, we have assumed that $\int_0^\infty q_i^2(s, \tau)d\tau \neq 0$ for any value of \bar{n} . On the other hand, for $\bar{n} \gg 1$, $\int_0^\infty q_i^2(s, \tau)d\tau \approx 0$ for $i = \{1, 2\}$, i.e the integral of approaches zero monotonically. Notice that each $q_i(s, \tau)$ for the DPO resembles the generating function $Q(s, \tau)$ for thermal

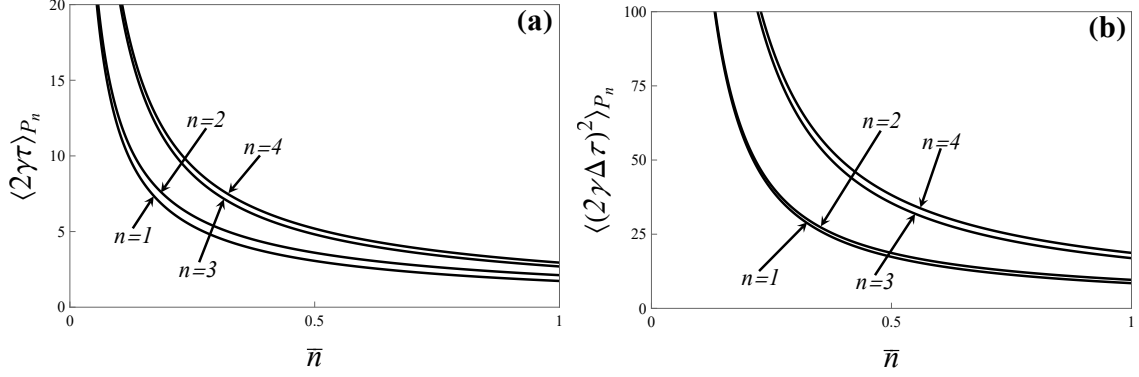


Figure 5.3: Unconditional average and variance of wait time τ for the photodetections $n = 1 - 4$ for the DPO case. As was the case for the plots for curves for thermal light we do not include averages and variances with respect to w_n .

light but taken as $\sqrt{Q(s, \tau)}$. Performing the integration of $\sqrt{Q(s, \tau)}$ is substantially harder than performing the integration of $Q(s, \tau)$. Instead, one sees that in the small mean photon number regime, the functional forms of $q_1(s, x)q_2(s, y)$ and $q_1(s, y)q_2(s, x)$ (Eq. (5.33)) become increasingly similar so the error e above becomes very small. A Mathematica script numerically proves this assertion. Since we already calculated quantities related to integration of $Q(s, \tau)$, in principle we have nothing new to do but to realize that the integration of $q_i^2(s, \tau)$ is the same as $Q(s, \tau)$ for thermal light. The expressions for the unconditional and conditional mean and variance of wait time are given as follows:

$$\begin{aligned} \langle \tau \rangle_{P_n} &= \frac{2}{\sqrt{\lambda_1 \lambda_2}} \sum_{k=0}^{n-1} \frac{(-1)^k}{k!} \frac{d^k}{ds^k} \varrho_1(s) \Big|_{s=1}, \\ \langle \tau^2 \rangle_{w_n} &= \frac{2}{\gamma \eta \bar{n} \sqrt{\lambda_1 \lambda_2}} \sum_{k=0}^{n-1} \frac{(-1)^k (n-k)}{k!} \frac{d^k}{ds^k} \varrho_1(s) \Big|_{s=1}, \end{aligned}$$

and

$$\langle \tau^2 \rangle_{P_n} = \frac{2}{\lambda_1 \lambda_2} \sum_{k=0}^{n-1} \frac{(-1)^k}{k!} \frac{d^k}{ds^k} \varrho_2(s) \Big|_{s=1},$$

where $\varrho_1(s, T)$ and $\varrho_2(s, T)$ take a very peculiar form:

$$\varrho_1(s) = \left(\frac{z_1}{\lambda_1} + 1 \right)^{-1} \left(\frac{z_2}{\lambda_2} + 1 \right)^{-1} \sqrt{\Phi(A_1, 1, B_1) \Phi(A_2, 1, B_2)} \quad (5.34)$$

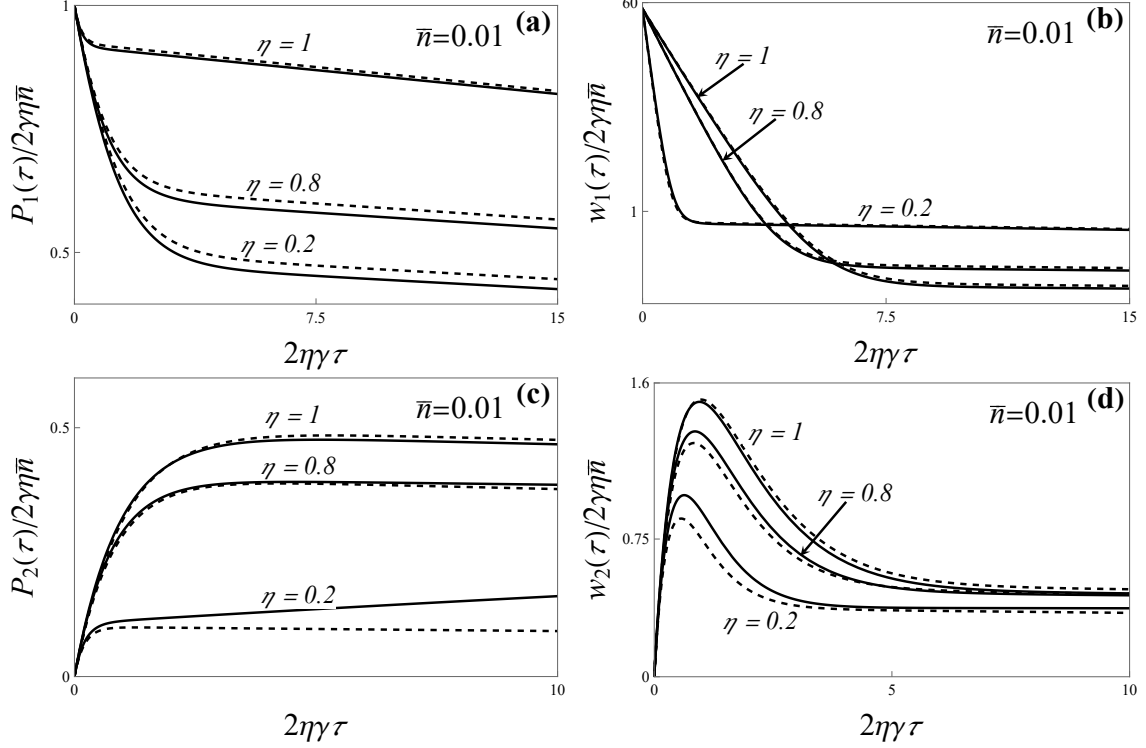


Figure 5.4: Effect of the non-unit detection efficiency. Exact curves for $P_n(\tau)$ and $w_n(\tau)$ for squeezed light from a DPO for $n = 1-3$ compared with approximate expressions (dashed curves) given by Eqs. (5.37)-(5.40) for $\bar{n} = 0.01$.

and

$$\varrho_2(s) = \left(\frac{z_1}{\lambda_1} + 1 \right)^{-1} \left(\frac{z_2}{\lambda_2} + 1 \right)^{-1} \sqrt{\frac{\Phi(A_1, 1, B_1)\Phi(A_2, 1, B_2)}{z_1 z_2}}. \quad (5.35)$$

Where

$$A_i = \left(\frac{z_i - \lambda_i}{z_i + \lambda_i} \right)^2, \quad B_i = \frac{z_1 + z_2 - 2\gamma}{2z_i}. \quad (5.36)$$

Φ are already known from the chapter on thermal light as Lerch's functions [37]. We will not discuss any further the mean and variance since it is not of high interest at time being, but perhaps deeper meaning can be withdrawn from these approximations. However, we remark the pairing of photons becomes noticeable in the small mean photon number limit. This behavior is shown in Figure 5.3.

5.4 Effect of Non-Unit Detection Efficiency

Non-unit detection efficiency ($\eta < 1$) causes the observed photo-detection sequence to differ from the photoemission sequence. The most significant effect of the non-unit detection efficiency for the DPO is to degrade the even-odd oscillations in the photo-count distribution. This has been discussed in detail in Ref. [30]. For non-unit detection efficiency the expressions for $P_n(\tau)$ and $w_n(\tau)$ for arbitrary n do not have simple forms. For large mean cavity photon number \bar{n} , the dominant effect of detection efficiency is already contained in expressions (5.28) and (5.30) and is similar to that found for thermal light in the high degeneracy limit [19].

For small \bar{n} where quantum effects dominate, the effect of detector efficiency is more interesting and illustrates how the quantum nature of photo-emission sequence can be obscured in the photo-detection sequence. As noted earlier, wait time distributions beyond $n = 1$ and 2 carry little qualitatively new information. Therefore, we will limit our considerations of non-unit detection efficiency to $n = 1, 2$ wait time distributions. Following a procedure similar to that used in arriving at Eqs. (5.19)- (5.24), we expand the generating function $G(s, \tau) = Q_1(s, \tau)Q_2(s, \tau)$ in powers of \bar{n} and retain terms necessary to satisfy the constraints of Eqs. (2.34) and (2.35). We then obtain the following expressions

$$P_1(\tau) = 2\eta\gamma\bar{n}e^{-(2\eta-\eta^2)\gamma\bar{n}\tau}\frac{1}{2}[2 - \eta + \eta e^{-2\gamma\tau}] \quad (5.37)$$

$$P_2(\tau) = 2\eta\gamma\bar{n}e^{-(2\eta-\eta^2)\gamma\bar{n}\tau}\frac{\eta}{2}[1 - e^{-2\gamma\tau}] \quad (5.38)$$

$$w_1(\tau) = 2\eta\gamma\bar{n}e^{-(2\eta-\eta^2)\gamma\bar{n}\tau}\frac{\eta}{2}\left[\frac{1}{4}(\eta - 2)^2 + \eta^2 e^{-4\gamma\tau} + e^{-2\gamma\tau}\left(2 + \frac{1}{2\bar{n}} + \eta - \frac{5\eta^2}{4}\right)\right] \quad (5.39)$$

$$w_2(\tau) = w_1(\tau) = 2\eta\gamma\bar{n}e^{-(2\eta-\eta^2)\gamma\bar{n}\tau}\frac{\eta}{2}[2 - \eta + 4\eta e^{-\gamma\tau} + e^{-2\gamma\tau}(5\eta - 6\eta\gamma\tau + 14\gamma\tau - 2)]. \quad (5.40)$$

As a check, we note that for $\eta = 1$, these expressions reduce to those in Eqs. (5.19)- (5.24) and satisfy the constraints on Eqs. (2.34) and (2.35). Figure 5.4 illustrates the effect of non-unit detection efficiency on wait time distributions. The full curves represent numerical

calculations using the generating function (5.10) in Eqs. (2.26) and (2.28). The dashed curves are obtained from Eqs. (5.37)-(5.40). Note that as η decreases, the two distinct time scales so prominent in the ideal case $\eta = 1$ slowly disappear and are replaced by a single time scale. We can also see analytically from the exponential before the square brackets that for small detection efficiency, the exponent $(2\eta - \eta^2)\gamma\bar{n}\tau \rightarrow 2\eta\gamma\bar{n}$. In this quantum regime, the detection efficiency changes the time scales as well as the shape of the distributions. As the detection efficiency decreases, the observed wait time distribution resembles a rate limited distribution for a classical field. Here we have an analytical model that allows us to see how the quantum mechanical properties of a photon sequence are washed out in the photo-count distribution with decreasing detection efficiency.

Chapter 6

Photon Counting Statistics of Resonance Fluorescence of Two Level Atom

Consider now the photon sequence produced by a single coherently driven two level atom near resonance. This is perhaps one of the most peculiar examples of a light source that requires a full quantum mechanical description to accurately characterize all its properties. With the emission of each photon, the atom returns to its lowest energy state, and so each subsequent photon-emission occurs with the atom starting in the lowest energy state independent of the history of previous photo-emissions. The driving field, being in a classical (coherent) state, remains unaffected by photo-emission events. Thus the photo-emissions from a coherently driven single two level atom form a time series that can be described as a Markov birth process [8, 10, 14, 17, 23, 38–40]. This property allows the averages of products of photon-flux operators over disjoint sub-intervals of a counting time interval $[0, \tau]$ to be simplified and expressed in terms of the products of two point correlation of the field intensity.

In the case of resonance fluorescence from a two level atom, it is convenient to use the forms for unconditional and conditional wait times distributions as given by Eqs. (2.31) and (2.32).

The integrand of (2.32) can be interpreted as the joint probability of detecting photons at the successive times $0, t_1, t_2, \dots, t_{k+n-1}, \tau$ [8, 23]. Recognizing the Markov property of photon-emissions the integrand of Eq. (2.32) can be rewritten as a product series of two-time conditional probabilities as follows [8, 41]. The conditional probability of a photo-detection at t_k conditioned upon a photo-detection at $t_{k-1} (< t_k)$ depends only on the interval $t_k - t_{k-1}$ and has the form

$$2\beta f_0(t_k - t_{k-1}) = \frac{\langle \mathcal{T} : \hat{I}(t_k) \hat{I}(t_{k-1}) : \rangle}{\langle \hat{I}(t_{k-1}) \rangle}, \quad (6.1)$$

where 2β is the Einstein A coefficient. A coefficient for the atomic transition. The integrand

of Eq. (2.32) can then be written as

$$\langle \mathcal{T} : \hat{I}(t_{n+k}) \hat{I}(t_{k+n-1}) \dots \hat{I}(t_1) \hat{I}(t_0) : \rangle = \langle \hat{I}(t_0) \rangle \prod_{j=0}^{k+n-1} 2\beta f_0(t_{j+1} - t_j), \quad (6.2)$$

where $\tau = t_{n+k}$ and $t_0 = 0$. Using Eqs. (6.10)-(6.2) and taking the Laplace transform [25] of the resultant expression, we obtain

$$\tilde{w}_n(s) = \sum_{k=0}^{\infty} \frac{(k+n-1)!(-1)^k}{(n-1)!k!} [2\beta\eta\tilde{f}_0(s)]^{k+n},$$

where $\tilde{w}_n(s)$ and $\tilde{f}_0(s)$ are the Laplace transforms of $w_n(\tau)$ and $f_0(t_{k+1} - t_k)$ respectively.

The sum in the preceding expression can be carried out leading to

$$\tilde{w}_n(s) = \left[\frac{2\beta\eta\tilde{f}_0(s)}{1 + 2\beta\eta\tilde{f}_0(s)} \right]^n. \quad (6.3)$$

The function \tilde{f}_0 is given by [8, 22, 23, 41],

$$\tilde{f}_0(s) = \frac{\Omega^2}{2s((s+2\beta)(s+\beta) + \Omega^2)}, \quad (6.4)$$

where Ω is the Rabi frequency for the atomic transition. $\tilde{w}_n(s)$ can be written directly in terms of atomic parameters as

$$\tilde{w}_n(s) = \left[\frac{\beta\eta\Omega^2}{s(s+\beta)(s+2\beta) + \Omega^2(s+\beta\eta)} \right]^n. \quad (6.5)$$

The factorization of the intensity correlation function also allows us to obtain a closed form expression for the Laplace transform of $P_n(\tau)$. Starting with the definition of Eq. (2.31) of $P_n(\tau)$, just like we did for $w_n(\tau)$, the integrand of Eq. (2.31) can be expressed in terms of a product series of intensity correlation functions of the form

$$\langle \mathcal{T} : \hat{I}(t_{n+k}) \hat{I}(t_{n+k-1}) \dots \hat{I}(t_1) : \rangle = (2\beta)^{n+k} (f(t_1)) \prod_{j=1}^{n+k-1} f(t_{j+1} - t_j), \quad (6.6)$$

where $f(t_1)$ is the probability of photo-emission given the atoms starts in the steady state [23].

After using Eq. (6.6) in Eq. (2.31), a formal Laplace transform of $P_n(\tau)$ yields

$$\tilde{P}_n(s) = 2\eta\beta\tilde{f}(s) \sum_{k=0}^{\infty} \frac{(-1)^k (n+k-1)!}{(n-1)!k!} [2\eta\beta\tilde{f}_0(s)]^{n+k-1},$$

with $\tilde{f}_0(s)$ given by Eq. (6.4) and the Laplace transform of $f(t_1)$ given by

$$\tilde{f}(s) = \frac{\Omega^2}{2s(\Omega^2 + 2\beta^2)}. \quad (6.7)$$

Above, we have a new function, which is the Laplace transform of $f(t_1)$. The summation above is in principle the same as for the case of $\tilde{w}_n(s)$. The exact expression for $\tilde{P}_n(s)$ is then

$$\tilde{P}_n(s) = \left[\frac{\tilde{f}(s)}{\tilde{f}_0(s)} \right] \left[\frac{2\eta\beta\tilde{f}_0(s)}{1 + 2\eta\beta\tilde{f}_0(s)} \right]^n. \quad (6.8)$$

It is convenient to have $\tilde{f}(s)/\tilde{f}_0(s) = \frac{s(s+3\beta)}{\Omega^2+2\beta^2} + 1$ so that $\tilde{P}_n(s) = (Cs^2 + 3\beta Cs + 1)\tilde{w}_n(s)$, where we have set the constant $C = \frac{1}{\Omega^2+2\beta^2}$. In addition, it can be shown from the definition of $w_n(\tau)$ from Eqs. (2.22) that $w_n(0) = 0$ and $w'_n = 0$ for all $n \geq 0$ and we will demonstrate this further on this section when we obtain an analytic expression for $w_n(\tau)$ in terms of atomic parameters. We can the rewrite the Laplace transform of $P_n(\tau)$ as

$$\tilde{P}_n(s) = C(s^2\tilde{w}_n(s) - sw_n(0^+) - w'_n(0^+)) + 3\beta C(s\tilde{w}_n(s) - w_n(0^+)) + \tilde{w}_n(s).$$

Where 0^+ signifies approaching zero from right to left. The above is only valid for resonance fluorescence from the two level atom and not for any other quantum system. The previous equation works out perfectly since it has an exact inverse Laplace transform in terms of $w_n(\tau)$. The inverse Laplace transform of $\tilde{P}_n(s)$ can be obtained by using a Bromwich integral [25] and yields

$$\begin{aligned} P_n(\tau) &= C\mathcal{L}^{-1}\{s^2\tilde{w}_n(s) - sw_n(0^+) - w'_n(0^+)\} + 3\beta C\mathcal{L}^{-1}\{s\tilde{w}_n(s) - w_n(0^+)\} + \mathcal{L}^{-1}\{\tilde{w}_n(s)\} \\ &= C\frac{d^2}{d\tau^2}w_n(\tau) + 3\beta C\frac{d}{d\tau}w_n(\tau) + w_n(\tau). \end{aligned} \quad (6.9)$$

The symbol \mathcal{L}^{-1} is the inverse Laplace transform operation. The expression for $P_n(\tau)$ is given in terms of $w_n(\tau)$ and knowing $w_n(\tau)$ will determine completely the form of $P_n(\tau)$.

This is the reason why on this section we have decided to begin our discussion of resonance fluorescence with $w_n(\tau)$ instead of $P_n(\tau)$. From the above formulas we can also have an exact expression for the parameter $g_n(\tau)$.

6.1 Unit Detection Efficiency $\eta = 1$

For unit quantum efficiency, the inverse Laplace transform of $\tilde{w}_n(s)$ (Eq. (6.5)) can be evaluated using calculus of residues yielding

$$w_n(\tau) = \frac{(\beta\Omega^2)^n}{((n-1)!)^3(\beta^2 - \Omega^2)^n} e^{-\beta\tau} \times \sum_{k=0}^{n-1} \tau^{n-k-1} [(-1)^n \mathcal{D}_0(n, k) + \mathcal{D}(n, k)((-1)^k e^{\sqrt{\beta^2 - \Omega^2}\tau} + e^{-\sqrt{\beta^2 - \Omega^2}\tau})], \quad (6.10)$$

where

$$\mathcal{D}_0(n, k) = \binom{n-1}{k} \frac{1}{(\sqrt{\beta^2 - \Omega^2})^k} \sum_{j=0}^k (-1)^j \binom{k}{j} (n+k-j-1)!(n+j-1)! \quad (6.11)$$

and

$$\mathcal{D}(n, k) = \binom{n-1}{k} \frac{1}{(\sqrt{\beta^2 - \Omega^2})^k} \sum_{j=0}^k \binom{k}{j} \frac{(n+k-j-1)!(n+j-1)!}{2^{n+j}}. \quad (6.12)$$

In general the above expressions must be evaluated numerically. Nevertheless, it can be seen from the form of the above equations that $w_n(0) = 0$ and $w'_n(\tau) = 0$. The result $w_1(0) = 0$ is, of course, the signature of well known photon anti-bunching. Numerical evaluation of Eq. (6.10) requires some care as the nature of the functions changes as the Rabi frequency varies from $\Omega < \beta$ to $\Omega > \beta$. Simpler expressions can be derived that provide a more intuitive picture of photon sequences generated. These will be taken next.

Let us write the exact expressions for the conditional wait time distribution $w_n(\tau)$ for

$n = 1-4$ when we use Eqs. (6.10)-(6.12). They take the following form:

$$w_1(\tau) = C_1 \beta e^{-\beta\tau} \left[-1 + \cosh(\omega\tau) \right], \quad (6.13)$$

$$w_2(\tau) = \frac{C_2}{2} \beta^2 \tau e^{-\beta\tau} \left[2 + \cosh(\omega\tau) - 3 \frac{\sinh(\omega\tau)}{\omega\tau} \right], \quad (6.14)$$

$$w_3(\tau) = \frac{C_3}{8} \beta^3 \tau^2 e^{-\beta\tau} \left[-4 + \cosh(\omega\tau) - 9 \frac{\sinh(\omega\tau)}{\omega\tau} + 24 \frac{\cosh(\omega\tau) - 1}{(\omega\tau)^2} \right], \quad (6.15)$$

and

$$w_4(\tau) = \frac{C_4}{3 \cdot 2^4} \beta^4 \tau^3 e^{-\beta\tau} \left[8 + \cosh(\omega\tau) - 18 \frac{\sinh(\omega\tau)}{\omega\tau} + \frac{3}{(\omega\tau)^2} \left(64 + 41 \cosh(\omega\tau) - 105 \frac{\sinh(\omega\tau)}{\omega\tau} \right) \right], \quad (6.16)$$

where $C_n = \frac{(\Omega/\beta)^{2n}}{(1-(\Omega/\beta)^2)^n}$ and $\omega = \sqrt{\beta^2 - \Omega^2}$. For weak driving fields, $\frac{\Omega^2}{\beta^2} \ll 1$ simple expressions for $w_n(\tau)$, similar to Eqs. (6.13)-(6.16) can be obtained in the long and short time regimes. In the short time regime $2\beta\tau \ll 1$, it is possible to use the approximation $\omega \approx \beta$ in the expressions for Eqs. (6.13)-(6.16). Observe that for $n = 1$ the distribution $w_1(\tau) \propto (1 - e^{-\beta\tau})^2$. The factor $(1 - e^{-\beta\tau})^2$ is related to the second order correlation function $g^{(2)}(\tau)$ which vanishes at $\tau = 0$ reflecting photon antibunching. In the case $n > 1$ relations between $w_n(\tau)$ and $g^{(n+1)}(\tau)$ can be found exactly.

Regarding the general approximation for a weak field, $\omega \approx \beta - \frac{\beta}{2} \frac{\Omega^2}{\beta^2}$ for all waiting times τ , plots and computations suggest that the distributions $w_n(\tau)$ and $P_n(\tau)$ resemble very closely that of a coherent field. In fact we used approximations for fluorescence of the two level atom against coherent light and the curves seem to have an overall resemblance across a wide range of waiting times τ [2, 7].

In the special case $\Omega = \beta$, it is simpler to use Eq. (6.5), which simplifies to $\tilde{w}_n(s) = \frac{\beta^{3n}}{(s+\beta)^{3n}}$ and its inverse Laplace transform is

$$w_n(\tau) = \beta \frac{(\beta\tau)^{3n-1}}{(3n-1)!} e^{-\beta\tau}. \quad (6.17)$$

The above is not quite a Poisson distribution but a Gamma distribution [25] with shape

parameter $3n$ and rate β .

It is interesting to compare Eq. (6.17) to the expressions for coherent light of the same mean photon-flux. Eq. (6.17) attains a maximum at the most probable time $\tau_{n,rf}^w = (3n - 1)\beta^{-1}$ which in terms of steady-state photon emission rate $\langle \hat{I} \rangle_{ss} = \beta/3$ can be written as $\tau_{n,rf}^w = (n - 1/3)\langle \hat{I} \rangle_{ss}^{-1}$. The corresponding most probable time for coherent light is $\tau_{n,ch} = (n - 1)\langle \hat{I} \rangle_{ss}^{-1}$. Since $\tau_{n,rf}^w = \tau_{n,coh} + (2/3)\langle \hat{I} \rangle_{ss}^{-1}$, we see that the most probable times for wait times in resonance fluorescence produced by a two level atom, on average, are longer than the most probable times for randomly distributed photons.

In the strong field regime $\frac{\Omega^2}{\beta^2} \gg 1$ and wait times that are not so small ($2\beta T > 1$), one can neglect the tail of the sum of Eq. (6.10). It is also worth mentioning that $\langle \hat{I} \rangle_{ss} = \frac{\beta\Omega^2}{\Omega^2 + 2\beta^2} \approx \beta$. Hence, $w_n(\tau)$ takes the form

$$w_n(\tau) \approx \beta \frac{(\beta\tau)^{n-1} e^{-\beta\tau}}{(n-1)!} \left[1 - \frac{(-1)^{n-1}}{2^{n-1}} \cos(\Omega\tau) \right]. \quad (6.18)$$

The error in Eq. (6.18) is of order $\mathcal{O}((\Omega/\beta)^{-1})$. A comparison of equation Eq. (6.18) with the result of Eq. (3.3) for coherent light shows that in this limit, $w_n(\tau)$ for resonance fluorescence is the product of the wait time coherent light distribution modulated by an oscillatory term due to Rabi oscillations. Figs. 6.1-(e) and 6.1-(f) show a good agreement between Eq. (6.18) and the exact expressions. On the other end, in the small time regime $2\beta\tau \ll 1$, it is sufficient to use expressions such as Eqs. (6.13)-(6.16) and Taylor expand the terms in square brackets to obtain physically meaningful expressions. After some work, it can be seen that the leading term for $w_n(\tau)$ is

$$w_n \propto \frac{\Omega^{2n}}{\beta^{2n}} \beta \frac{(\beta\tau)^{3n-1}}{(3n-1)!} e^{-\beta\tau}. \quad (6.19)$$

For very short times, the conditional wait time distribution $w_n(\tau)$ is dominated by a gamma distribution similar to the case $\Omega = \beta$ given by Eq. (6.17) times the term $\frac{\Omega^{2n}}{\beta^{2n}}$. We notice that Eq. (6.19) is meaningless as a distribution since it is not truly a probability but just a leading order for small wait times and large fields. If we take Eq. (6.19) as a probability

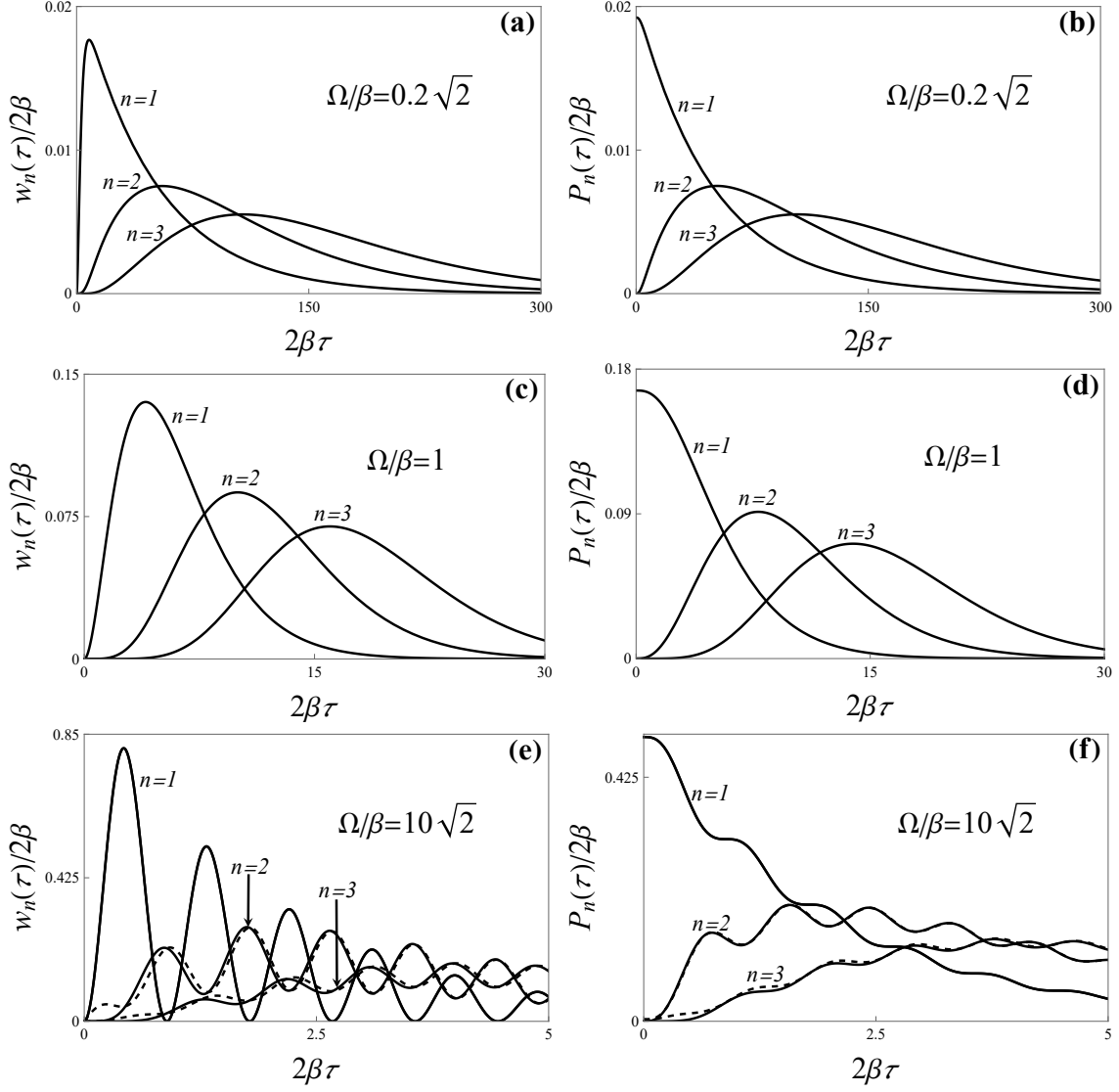


Figure 6.1: $w_n(\tau)$ and $P_n(\tau)$ for small ($\Omega/\beta = 0.2\sqrt{2}$ sub-figures (a)-(b)), resonant ($\Omega/\beta = 1$ sub-figures (c)-(d)), and large ($\Omega/\beta = 10\sqrt{2}$, sub-figures (e)-(f)) driving fields for $n = 1 - 4$. The dashed curves in sub-figures (e) and (f) represent large field approximations, see Eq.(6.18).

distribution we will have to normalize it to unity in which case we get the same equation for the case $\Omega = \beta$.

Consider now the unconditional wait time distribution $P_n(\tau)$. Taking the inverse Laplace transform of Eq. (6.8) or using Eq. (6.9) and Eqs. (6.10)-(6.12) a similar expression to $w_n(\tau)$ can be derived for $P_n(\tau)$. Since the expressions for $P_n(\tau)$ resemble quite closely those for $w_n(\tau)$ we omit writing all the cases explicitly here. We write only the case $\Omega = \beta$ which is

given by

$$P_n(\tau) = \frac{\beta (\beta\tau)^{3(n-1)}}{3 (3n-1)!} e^{-\beta\tau} [((\beta\tau)^2 + (3n-1)\beta\tau + (3n-1)(3n-2))]. \quad (6.20)$$

The above formula satisfies $P_1(0) = \frac{\beta}{3}$. Eq. (6.20) is plotted in Figs. 6.1-c and 6.1-d. For the small and large field regimes it suffices to use the formulas for $w_n(\tau)$ we have already discussed. All the exact expressions and approximations for different cases of the exciting/driving field are plotted on Figs. (8)-(10). Calculations of $P_n(\tau)$ also allow us to find the deficiency correlation $g_n(\tau)$. For brevity, consider only the case $\Omega = \beta$, $w_n(\tau)$ and $P_n(\tau)$ are very simple functions so then

$$g_n(\tau) = \frac{3(\beta\tau)^2}{(\beta\tau)^2 + (3n-1)\beta\tau + (3n-1)(3n-2)}. \quad (6.21)$$

Notice immediately that for short times $\beta\tau$, $g_n(\tau) < 1$, which is the anti-bunching property of resonance fluorescence. Also notice that for some values of $\beta\tau$, $g_n(\tau) > 1$ and $g_n(\tau)$ approaches 3 as $\beta\tau \gg 1$. For small fields, $g_n(\tau)$ is always less than 1 and approaches 1 as wait times increase. The case for a large field exhibits Rabi oscillations. These oscillations happen around 1 and their amplitude decreases as n increases.

6.2 Non-Unit Detection Efficiency Effect

For non-unit detection efficiency, the expressions for $w_n(\tau)$ and $P_n(\tau)$ become cumbersome. However, we can write down auxiliary definitions that make $w_n(\tau)$ and $P_n(\tau)$ look more appealing. Let us start by considering the denominator of Eq. (6.5), $s(s + \beta)(s + 2\beta) + \Omega^2(s + \eta\beta)$. It can be factored as $(s - s_1)(s - s_2)(s - s_3)$ where s_1, s_2 and s_3 can be found using Cardano's formula. The resulting expressions for the roots are

$$s_1 = -\beta + \Delta_1 + \Delta_2 \quad (6.22)$$

$$s_2 = -\beta - \Delta_1 e^{i\pi/3} - \Delta_2 e^{-i\pi/3} \quad (6.23)$$

$$s_3 = -\beta - \Delta_1 e^{-i\pi/3} - \Delta_2 e^{i\pi/3}. \quad (6.24)$$

Where

$$\Delta_1 = \frac{\omega^2}{\delta}, \quad \Delta_2 = \frac{1}{3}\delta, \quad \delta = \frac{B}{\sqrt[3]{2}}, \quad \omega^2 = \beta^2 - \Omega^2,$$

$$B = [27\beta(1 - \eta)\Omega^2 + \sqrt{4 \cdot 27(\Omega^2 - \beta^2)^3 + (27\beta(1 - \eta)\Omega^2)^2}]^{1/3}.$$

Note that the expressions for $\Delta_1, \Delta_2, \delta$ and ω have units of frequency.

In the case that $\eta = 1$, observe that $B = \sqrt[3]{2}\sqrt{3(\Omega^2 - \beta^2)}$, then we recover $s_1 = -\beta$, $s_2 = -\beta - \sqrt{\beta^2 - \Omega^2}$ and $s_3 = -\beta + \sqrt{\beta^2 - \Omega^2}$. This leads to the already known expressions for $w_n(\tau)$ and $P_n(\tau)$.

Following the method we described in previous sections, we can also find the expression for the conditional wait time distribution in the non-unit detection efficiency case. It follows that

$$w_n(\tau) = C_n e^{-\beta\tau} \times$$

$$\sum_{k=0}^{n-1} \binom{n-1}{k} \frac{\tau^{n-1-k}}{(\sqrt{3(\Delta_1^2 + \Delta_1\Delta_2 + \Delta_2^2)})^k} [(-1)^k \mathcal{J}_0(n, l) e^{\Delta_1\tau + \Delta_2\tau} + 2(-1)^n \mathcal{J}(n, l, \tau) e^{-\frac{\Delta_1 + \Delta_2}{2}\tau}].$$
(6.25)

Where in the above we have defined :

$$\omega = \sqrt{\beta^2 - \Omega^2}, \quad C_n = \frac{(\eta\beta\Omega^2)^n}{((n-1)!3^{3n}(\Delta_1^2 + \Delta_1\Delta_2 + \Delta_2^2))^n},$$

$$\mathcal{J}_0(n, k) = \sum_{p=0}^k \binom{k}{p} (n+k-p-1)!(n+p-1)! \cos((2p-k)\theta_1),$$

$$\mathcal{J}(n, k, \tau) = (\sqrt{3}) \left[\frac{\sqrt{\Delta_1^2 + \Delta_1\Delta_2 + \Delta_2^2}}{\Delta_2 - \Delta_1} \right]^n \times$$

$$\sum_{p=0}^k \binom{k}{p} (-1)^p (n+k-p-1)!(n+p-1)! \left[\frac{\sqrt{\Delta_1^2 + \Delta_1\Delta_2 + \Delta_2^2}}{\Delta_2 - \Delta_1} \right]^p \cos \left[\frac{\Delta_2 - \Delta_1}{2} \sqrt{3}\tau + \phi_{nkp} \right],$$

$$\theta_1 = \arctan \left[\frac{1}{\sqrt{3}} \frac{\Delta_2 - \Delta_1}{\Delta_2 + \Delta_1} \right] \quad \text{and} \quad \phi_{nkp} = \theta_1(n+k-p) - (n+p) \frac{\pi}{2}.$$
(6.26)

See Figs. 6.2 for the effect of the non-unit detection efficiency in both distributions w_n and P_n . Consider expressions for some special cases and some approximations for the conditional

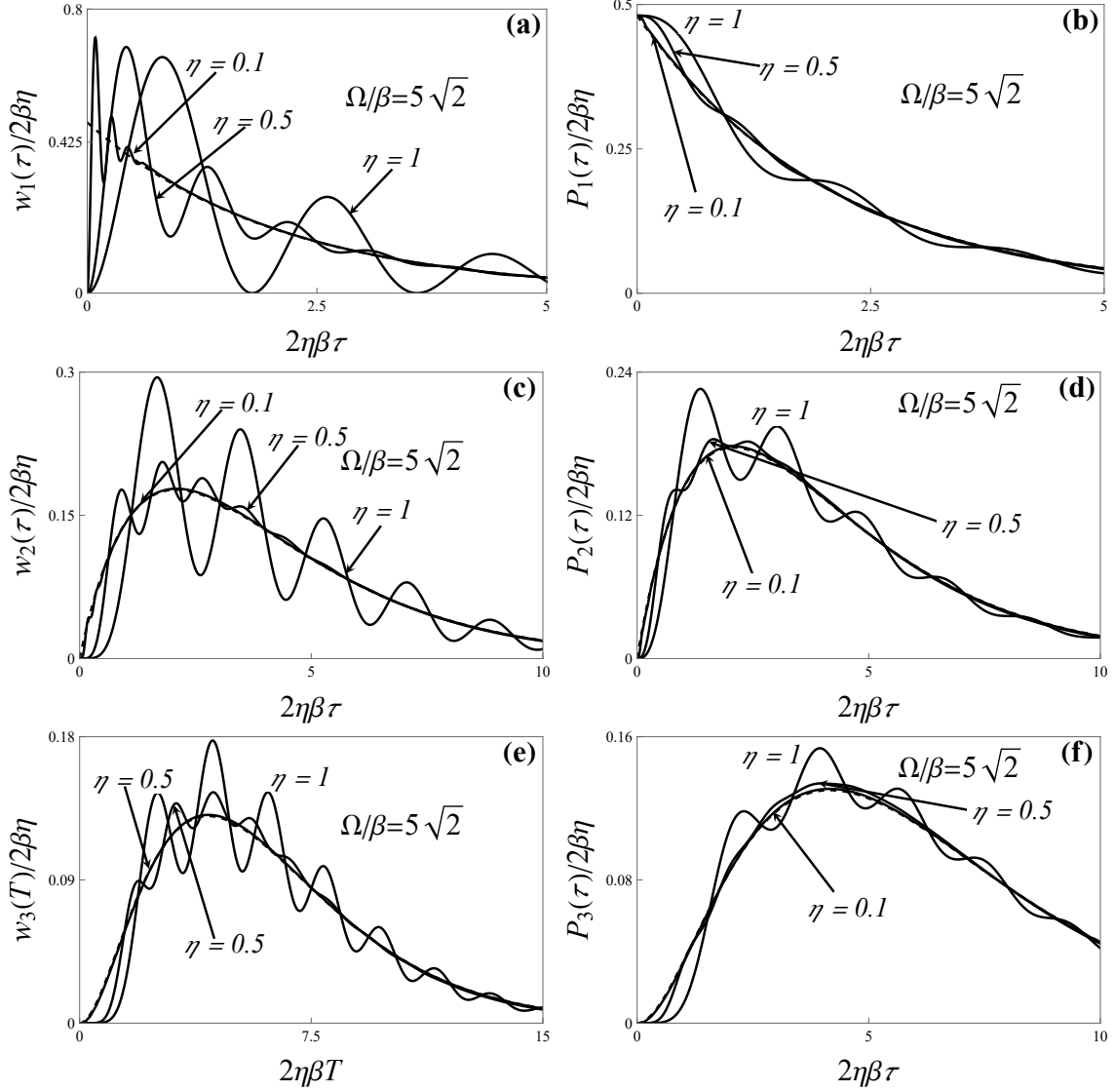


Figure 6.2: Effect of the non-unit detection efficiency on unconditional waiting time distributions for resonance fluorescence for $n = 1 - 4$. The distribution approach the coherent limit as η decreases, this can be seen through figures (a)-(e) where the dashed curve represents coherent light.

and unconditional wait times distributions. For instance, $w_n(\tau)$ for the first photoelectric detection is given as

$$w_1(\tau) = \frac{\eta\beta\Omega^2 e^{-\beta\tau + (\Delta_1 + \Delta_2)\tau}}{3(\Delta_1^2 + \Delta_1\Delta_2 + \Delta_2^2)} \times \left[1 - 2 \frac{\sqrt{\Delta_1^2 + \Delta_1\Delta_2 + \Delta_2^2}}{\Delta_2 - \Delta_1} e^{-(\Delta_1 + \Delta_2)3\tau/2} \sin\left(\frac{\Delta_2 - \Delta_1}{2} \sqrt{3}\tau + \theta_1\right) \right]. \quad (6.27)$$

Suppose we take the limit $\Omega = \beta$ in Eq. (6.27). We then have that $\Delta_1 = 0$, $\Delta_2 = \beta\mu$ where $\mu = (1 - \eta)^{1/3}$, and $\theta_1 = \frac{\pi}{6}$. Then,

$$w_1(\tau) = \frac{\eta\beta}{3\mu^2} e^{-\beta\tau(1-\mu)} \left[1 - 2e^{-\frac{3}{2}\beta\mu\tau} \cos \left[\frac{\sqrt{3}}{2}\mu\beta\tau - \frac{\pi}{3} \right] \right]. \quad (6.28)$$

Furthermore, using Eq. (6.9) it follows that

$$P_1(\tau) = \frac{\eta\beta e^{-\beta\tau(1-\mu)}}{9\mu^2} \left[1 + \mu + \mu^2 - 2e^{-\frac{3}{2}\beta\mu\tau} \left[\left[1 - \frac{\mu}{2} - \frac{\mu^2}{2} \right] \cos \left[\frac{\sqrt{3}}{2}\mu\beta\tau - \frac{\pi}{3} \right] + \mu(\mu - 1) \frac{\sqrt{3}}{2} \sin \left[\frac{\sqrt{3}}{2}\mu\beta\tau - \frac{\pi}{3} \right] \right] \right]. \quad (6.29)$$

Observe that Eq. (6.29), is not 0 when $\tau = 0$. For $\eta \ll 1$, it follows that $w_1(\tau)/\eta \approx \frac{\beta}{3}g^{(2)}(\tau)$ and $P_1(\tau)/\eta \approx \frac{\beta}{3}$. Hence, we have that $g_1(\tau) \approx g^{(2)}(\tau)$. Therefore, the small quantum efficiency limit is equivalent to a small time approximation in our distributions. At $\tau = 0$, $g^{(2)}(0) = 0$. The previous findings agree with those of [8]. On an additional note, since $w_n(0) = 0$, the function $g_n(\tau)$ can be shown to always satisfy $g_n(0) = 0$ for any $n > 0$ in the non-unit detection efficiency case.

Consider the cases $\frac{\Omega^2}{\beta^2} \ll 1$ and $\frac{\Omega^2}{\beta^2} \gg 1$ when $\eta \sim 1$ (quantum efficiency is close to but not one) and the case $\eta \ll 1$ (the cases $B^3 < 0$, $B^3 = 0$, and $B^3 > 0$ have interesting implications but we do not mention those in these thesis since they deviate from our main scope). In the case $\eta \ll 1$, regardless of the strength of the field, the distributions for $w_n(\tau)$ and $P_n(\tau)$ are very close qualitatively to the distributions for coherent light, with the exception that $w_1(0) = 0$. When the field is small and the detection efficiency is not so small, we can still see that the anti-bunching effect of fluorescent photons has not been completely watched out, however, as either the field become weaker or quantum efficiency very small, one just expects a random photoelectric-count sequence.

Let us now discuss the strong field $\frac{\Omega^2}{\beta^2} \gg 1$ case and the unit detection efficiency not far from 1 when the wait time τ is not so small. In this case, we can use the very useful approximation $\Delta_1 \approx -\omega' + \delta$, $\Delta_2 \approx \omega' + \delta$ and $\theta_1 \approx \frac{\pi}{2}$, where we have defined $\omega' \approx -\frac{\Omega}{\sqrt{3}}$ and $\delta \approx \frac{\beta}{2}(1 - \eta)$. In principle, we can say that the fundamental frequencies Δ_1 and Δ_2

experience a shift due to the introduction of a non-unit detection efficiency in the strong field regime. It then follows by defining $\mathcal{R} = \Omega/\beta$ and $\xi = \frac{\sqrt{\mathcal{R}^2 + \frac{3}{4}(1-\eta)^2}}{\mathcal{R}}$ that $w_n(\tau)$ takes the form

$$w_n(\tau) = \frac{\eta^n \beta (\beta \tau)^{n-1} e^{-\beta \tau}}{(n-1)! \xi^{2n}} \left[e^{\beta(1-\eta)\tau} + (-1)^n \cos(\Omega \tau) e^{-\frac{1}{2}\beta(1-\eta)\tau} \frac{\xi^n}{2^{n-1}} \right] + \mathcal{O}(\mathcal{R}^{-1}) \quad (6.30)$$

Where again we assume the expression to be useful for times that are not so small. Setting $\eta = 1$ in the above expression gives Eq. (6.18) back. Additionally, to test that the distribution is close to normalization for strong fields, we have that integration of Eq.(6.30) yields

$$\frac{1}{\xi^{2n}} + 2 \left[\frac{-\eta}{\xi(3-\eta)\sqrt{1 + \frac{4\mathcal{R}^2}{(3-\eta)^2}}} \right]^n \cos \left[n \arctan \left(\frac{2\mathcal{R}}{3-\eta} \right) \right],$$

and it is straight forward to show that as $\mathcal{R} \gg 1$, $\xi \rightarrow 1$ and the above expression approaches 1. If it is desired, we can have Eq.(6.30) divided by the above normalization constant and use it as normalized $w_n(\tau)$. We want to remark that, even though one might have the ability to create a high-intensity driving field, the photoelectric detections are still dominated by η . As in the case of $\eta = 1$, Rabi oscillations die out when n increases according to Eq. (6.30). When the field is strong and the detection efficiency is very small, we then again get statistics that resemble that of coherent light. In the case of $P_n(\tau)$ refer to Figure 6.2 for the effect of non-unit detection on $P_n(\tau)$.

We can now compute the average of wait times and standard deviation for a resonance fluorescence from a two level atom. But first, let us make a quick diversion. We remark that in the case of thermal light and squeezed light from a DPO, the exact expressions for averages of wait times τ and τ^2 in terms $w_n(\tau)$ and $P_n(\tau)$ were rather complicated. Consequently, computation of average and variance of wait time τ were notoriously involved. As we will show in the remaining of this section, the computations for the mean and variance of wait time τ for the resonance fluorescence from a two level atom becomes more accessible since we have a close form for the Laplace transforms for $w_n(\tau)$ and of course $P_n(\tau)$. First, we desire to calculate the average of τ^m with respect to Eq. (6.10) where m denotes a positive integer

$m > 0$. There is a problem if we decide immediately integrate τ^m against Eqs. (6.10)-(6.12). The resulting expressions cannot be easily summed. However, an indirect way of finding the average of τ^m is given by

$$\langle \tau^m \rangle_{w_n} = (-1)^m \frac{\partial^m}{\partial s^m} \tilde{w}_n(s) \Big|_{s=0}, \quad (6.31)$$

where $\tilde{w}_n(s)$ is given by Eq. (6.5). Since we know exactly the form of $\tilde{w}_n(s)$ obtaining averages and variances for waiting times poses no challenge.

Consider first the case $\Omega = \beta$ and $\eta = 1$. We obtain that

$$\langle \tau^m \rangle_{w_n, \Omega=\beta} = \frac{m!}{\beta^m} \binom{3n+m-1}{m}. \quad (6.32)$$

Also, more generally

$$\langle \tau \rangle_{w_n} = \frac{n}{\eta \langle \hat{I} \rangle_{ss}}, \quad (6.33)$$

where $\langle \hat{I} \rangle_{ss} = \frac{\beta \Omega^2}{(\Omega^2 + 2\beta^2)}$ is the steady state mean photon-flux and

$$\langle \tau^2 \rangle_{w_n} = \frac{n}{(\eta \langle \hat{I} \rangle_{ss})^2} \left[n + 1 - \frac{6\eta\beta^2\Omega^2}{(\Omega^2 + 2\beta^2)^2} \right]. \quad (6.34)$$

This leads to the variance

$$\langle \Delta \tau^2 \rangle_{w_n} = \frac{n}{(\eta \langle \hat{I} \rangle_{ss})^2} \left[1 - \frac{6\eta\beta^2\Omega^2}{(\Omega^2 + 2\beta^2)^2} \right]. \quad (6.35)$$

Furthermore, we can obtain averages of wait times with respect to $P_n(\tau)$ by means of the formula

$$\langle \tau^m \rangle_{P_n} = \frac{m(m-1)}{(\Omega^2 + 2\beta^2)} \langle \tau^{m-2} \rangle_{w_n} - \frac{3\beta m}{(\Omega^2 + 2\beta^2)} \langle \tau^{m-1} \rangle_{w_n} + \langle \tau^m \rangle_{w_n}. \quad (6.36)$$

Above, it is evident that $\langle 1 \rangle_{P_n} = \langle 1 \rangle_{w_n}$, showing in fact that if $w_n(\tau)$ is normalized and so is $P_n(\tau)$.

Using the results above we have that the average of wait time and squared wait time

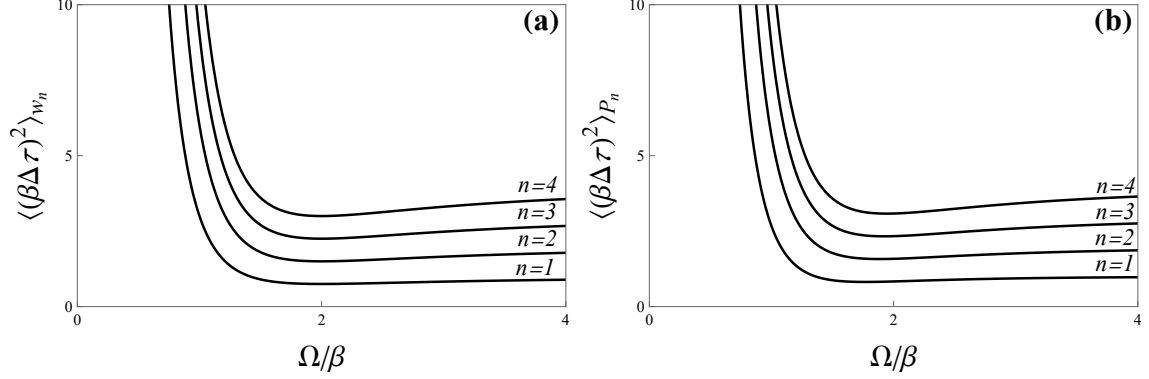


Figure 6.3: Conditional and Unconditional variance of wait time τ for the photodetections $n = 1 - 4$ for resonance fluorescence. Notice as in the large field limit, each variance approaches its corresponding n value.

with respect to $P_n(\tau)$ are

$$\langle \tau \rangle_{P_n} = \frac{n}{\eta \langle \hat{I} \rangle_{ss}} \left[1 - \frac{3\eta\beta^2\Omega^2}{n(\Omega^2 + 2\beta^2)^2} \right] \quad (6.37)$$

and

$$\langle \tau^2 \rangle_{P_n} = \frac{n(n+1)}{(\eta \langle \hat{I} \rangle_{ss})^2} + \frac{2}{\Omega^2 + 2\beta^2} \left[1 - \frac{6n\beta}{\eta \langle \hat{I} \rangle_{ss}} \right]. \quad (6.38)$$

The variance is therefore

$$\langle \Delta \tau^2 \rangle_{P_n} = \langle \Delta \tau^2 \rangle_{w_n} + \frac{2\Omega^2 - 5\beta^2}{(\Omega^2 + 2\beta^2)^2}. \quad (6.39)$$

From the above formulations, we note that for a very weak field $\frac{\Omega^2}{\beta^2} \ll 1$, $\langle \tau \rangle_{w_n}$, $\langle \tau \rangle_{P_n}$, $\langle \tau^2 \rangle_{w_n}$, and $\langle \tau^2 \rangle_{P_n}$ become very large giving rise to very large wait time variance with respect to both $w_n(\tau)$ and $P_n(\tau)$. This means that the two level atom that is not at all excited and the photo-emissions incident on the photo detector are very few, the average wait time for any of its n th photons becomes infinite since it is extremely unlikely the atom will be spontaneously excited and therefore it does not decay to its lowest energy state.

In the special case that $\Omega = \beta$, $\langle \Delta \tau^2 \rangle_{w_n} = \frac{3n}{\eta^2 \beta^2} (3 - 2\eta)$ which implies that $\langle \Delta \tau^2 \rangle_{w_n} >$

$\langle \Delta\tau^2 \rangle_{P_n}$. Lastly, we consider the strong field limit, $\frac{\Omega^2}{\beta^2} \gg 1$. Previous formulas indicate that

$$\lim_{\Omega/\beta \rightarrow \infty} \eta\beta \langle \tau \rangle_{w_n} = n, \quad (6.40)$$

$$\lim_{\Omega/\beta \rightarrow \infty} \eta^2 \beta^2 \langle \tau^2 \rangle_{w_n} = n(n+1). \quad (6.41)$$

These two limits lead to

$$\lim_{\Omega/\beta \rightarrow \infty} \eta^2 \beta^2 \langle \Delta\tau^2 \rangle_{w_n} = n. \quad (6.42)$$

For fields strong enough, we expect that the average time of detecting the n th photon is exactly the sum of n times the decay rate of a two level atom β^{-1} .

Chapter 7

Summary

7.1 Conclusion

We have discussed and introduced the concept of light field and its use in coherence functions. The coherence of all orders offer means for which an arbitrary light field can be tested theoretically and with development and effort one can experimentally show its true physical nature. Generally speaking, a light field does not necessarily have to be characterized as a stationary signal in the wide-sense but it may be thought of as any type of stochastic signal. We have remarked the importance of knowing which type of light signal one deals with, theoretically or experimentally, in order to explore the limitations of the theoretical apparatus used to understand light. Taking into consideration general statistical properties of any light signal, we have derived expressions that are of great help in order to approach the problem of describing the statistical properties related to time of a photon sequence as accurately as possible. Quantities such as the second order correlation functions and generating functions are necessary tools we have adapted to our work in order to facilitate the express understanding of other derived quantities that are essential in understanding the temporal statistics of photon sequences. These other quantities are factorial moments, photoelectric count probabilities, the Mandel's Q parameter, and generalized unconditional and conditional wait time distributions.

A large portion of this thesis, four entire chapters, were devoted to the generalized wait time distributions of an n th photoelectric detection. The wait time distributions are termed unconditional and conditional depending on how we have started our search for the n th photoelectric detection. If we begin the counting process of a photon sequence at an arbitrary time, the wait time distribution is defined as unconditional. If starting the counting process is restricted/conditioned to a first photoelectric detection, the wait time distribution is defined as conditional. Contrary to any normalized order of coherence, the wait time distributions

depend on the efficiency of detection. If the efficiency of a detector is perfect, then no distinction between photo-emission of a source and photo-detection needs to be made. On the other hand, the effect of a detection efficiency less than unity is to degrade the photon sequence by deleting photons from a photo-emission sequence randomly. For a very small detection efficiency, enough photons from a photo-emission sequence have been deleted so that in turn the photon-emission sequence is indistinguishable from one emitted by a coherent source.

Our treatment of generalized wait time distributions is first devoted to coherent light, thermal light, squeezed light from a degenerate parametric oscillator, and resonance fluorescence from a single coherently driven two level atom. We consider the source of thermal light to be a laser operating below threshold which allows us to place thermal light in the same footing for comparison with light from the degenerate parametric oscillator and light from the resonant fluorescent atom. On the same mark, the degenerate parametric oscillator is also assumed to be operating below threshold.

In all three cases we have mentioned, different regimes were explored. For example, for thermal light and the degenerate parametric oscillator, small and large mean photon number limits are considered, and expressions are derived correspondingly. In both cases, the small mean photon regime number reveals the pair like behavior of the photon sequence from both thermal light and the DPO. The pair-like property is carried over by both unconditional and unconditional wait time distributions and time averages with respect to wait times. The large mean photon number regime also reveals the bunching property of thermal and light from the DPO. In addition, for the case of the resonance fluorescence from a two level atom, small and large field regimes were also discussed. We have seen that as the field interacting with the two level atom becomes weaker the photon sequence emitted by the atom becomes random, coherent. On the other extreme, when the field is large, the wait time distributions are modulated by Rabi frequencies. Overall, the photon sequences produced by a coherently driven two level atom are shown to be anti-bunched as compared to the bunched photon

sequences of a single-mode laser operating below threshold and the sub-threshold DPO. We also discussed the effect of non-unit detection efficiency. In the case of thermal light and DPO and as well as the two level atom we see that as η decreases, the distributions approach that of coherent light. We note that deeper notion of the statistical properties of thermal light, light from the DPO, and resonance fluorescence from a two level atom can be extracted from both generalized unconditional and conditional wait time distributions for the *first*, *second*, *third*, and so on, photoelectric detection. We demonstrated that new insights can be gained due to the understanding of generalized unconditional and conditional wait times for each source of light as well as insights into their sub-Poissonian, Poissonian and super-Poissonian statistical descriptions.

7.2 Future Work

Part of my work was also based on the heterodyction of squeezed light from a DPO with that of a local oscillator which is purely coherent. We studied the transient and steady-state regimes for a heterodyne DPO. We will also work towards the description of the photon count probabilities, the generalized unconditional and the conditional wait time distributions for this source of light.

The current direction we hope to take is in the area of photonic quantum computing. This is so, since results found in my recent work could open the possibility to using of squeezed light from a DPO to perform heterodyction and possibly enhance certain features of the DPO photon sequence with the possibility of retaining statistical properties of the other photon sequence.

My hope is that I can continue a fruitful collaboration with professors Reeta Vyas and Surendra Singh and find out how useful heterodyction is in photonic quantum computing and quantum computing in general, specially using the DPO as main source of squeezed light. However, other sources of squeezing could be considered in order to demonstrate advantage as far as it goes on enhancing or retaining particular properties of a desired portion of a

photon sequence signal.

Bibliography

- [1] Leonard Mandel and Emil Wolf. *Optical coherence and quantum optics*. Cambridge university press, 1995.
- [2] R. Loudon. *The Quantum Theory of Light*. Clarendon Press, Oxford, second edition, 1983.
- [3] Gordon Baym. The physics of hanbury brown–twiss intensity interferometry: from stars to nuclear collisions, 1998.
- [4] Marlan O. Scully and M. Suhail Zubairy. *Quantum Optics*. Cambridge University Press, 1997.
- [5] Bahaa Saleh. *Photoelectron statistics: with applications to spectroscopy and optical communication*, volume 6. Springer, 2013.
- [6] L. MANDEL and E. WOLF. Coherence properties of optical fields. *Rev. Mod. Phys.*, 37:231–287, Apr 1965.
- [7] Cherif Bendjaballah and Francoise Perrot. Statistical properties of intensity-modulated coherent radiation. Theoretical and experimental aspects. *Journal of Applied Physics*, 44(11):5130–5141, 10 2003.
- [8] HJ Carmichael, Surendra Singh, Reeta Vyas, and PR Rice. Photoelectron waiting times and atomic state reduction in resonance fluorescence. *Physical Review A*, 39(3):1200, 1989.
- [9] Roy J Glauber. The quantum theory of optical coherence. *Physical Review*, 130(6):2529, 1963.
- [10] Howard Carmichael. *Statistical methods in quantum optics 1: master equations and Fokker-Planck equations*, volume 1. Springer Science & Business Media, 1999.
- [11] PD Drummond and CW Gardiner. Generalised p-representations in quantum optics. *Journal of Physics A: Mathematical and General*, 13(7):2353, 1980.
- [12] Wim C Van Etten. *Introduction to random signals and noise*. John Wiley & Sons, 2006.
- [13] Reeta Vyas and Surendra Singh. Antibunching and photoemission waiting times. *JOSA B*, 17(4):634–637, 2000.
- [14] Howard Carmichael. *An open systems approach to quantum optics: lectures presented at the Université Libre de Bruxelles, October 28 to November 4, 1991*, volume 18. Springer Science & Business Media, 2009.
- [15] Howard J Carmichael. *Statistical methods in quantum optics 2: Non-classical fields*. Springer Science & Business Media, 2009.
- [16] PL Kelley and WH Kleiner. Theory of electromagnetic field measurement and photoelectron counting. *Physical Review*, 136(2A):A316, 1964.

- [17] L. Mandel. Sub-poissonian photon statistics in resonance fluorescence. *Opt. Lett.*, 4(7):205–207, Jul 1979.
- [18] AB Dodson and Reeta Vyas. Homodyne photon statistics of the subthreshold degenerate parametric oscillator. *Physical Review A*, 47(4):3396, 1993.
- [19] Reeta Vyas and Surendra Singh. Waiting-time distributions in the photodetection of squeezed light. *Physical Review A*, 38(5):2423, 1988.
- [20] HF Arnoldus and G Nienhuis. Photon statistics of fluorescence radiation. *Optica Acta: International Journal of Optics*, 33(6):691–702, 1986.
- [21] Henk F Arnoldus and Robertsen A Riehle. Conditional probability densities for photon emission in resonance fluorescence. *Physics Letters A*, 376(38-39):2584–2587, 2012.
- [22] Henk F Arnoldus and Robertsen A Riehle. Waiting times, probabilities and the q factor of fluorescent photons. *Journal of Modern Optics*, 59(11):1002–1015, 2012.
- [23] D. Lenstra. Photon-number statistics in resonance fluorescence. *Phys. Rev. A*, 26:3369–3377, Dec 1982.
- [24] J. A. McFadden. On the lengths of intervals in a stationary point process. *Journal of the Royal Statistical Society. Series B (Methodological)*, 24(2):364–382, 1962.
- [25] George B Arfken, Hans J Weber, and Frank E Harris. *Mathematical methods for physicists: a comprehensive guide*. Academic press, 2011.
- [26] Hermann Haken. Laser theory. In *Light and Matter Ic/Licht und Materie Ic*, pages 1–304. Springer, 1984.
- [27] Gabriel Bédard. Photon counting statistics of gaussian light. *Physical Review*, 151(4):1038, 1966.
- [28] E Jakeman and ER Pike. The intensity-fluctuation distribution of gaussian light. *Journal of Physics A: General Physics*, 1(1):128, 1968.
- [29] Fredrik Brange, Paul Menczel, and Christian Flindt. Photon counting statistics of a microwave cavity. *Physical Review B*, 99(8):085418, 2019.
- [30] Reeta Vyas and Surendra Singh. Photon-counting statistics of the degenerate optical parametric oscillator. *Physical Review A*, 40(9):5147, 1989.
- [31] PD Drummond, KJ McNeil, and DF Walls. Non-equilibrium transitions in sub-second harmonic generation. *Optica Acta: International Journal of Optics*, 27(3):321–335, 1980.
- [32] M Wolinsky and HJ Carmichael. Quantum noise in the parametric oscillator: from squeezed states to coherent-state superpositions. *Physical review letters*, 60(18):1836, 1988.

- [33] Reeta Vyas and Surendra Singh. Quantum statistics of broadband squeezed light. *Optics letters*, 14(20):1110–1112, 1989.
- [34] Jianming Huang and Prem Kumar. Photon-counting statistics of multimode squeezed light. *Physical Review A*, 40(3):1670, 1989.
- [35] Milton Abramowitz and Irene A. Stegun. *Handbook of Mathematical Functions with Formulas, Graphs, and Mathematical Tables*. Dover, New York, ninth dover printing, tenth gpo printing edition, 1964.
- [36] A.N. Kolmogorov, S.V. Fomin, and S.V. Fomin. *Elements of the Theory of Functions and Functional Analysis*. Number v. 1 in Dover books on mathematics. Dover, 1999.
- [37] Jesús Guillera and Jonathan Sondow. Double integrals and infinite products for some classical constants via analytic continuations of lerch’s transcendent. *The Ramanujan Journal*, 16(3):247–270, jul 2008.
- [38] HJ Carmichael and DF Walls. A quantum-mechanical master equation treatment of the dynamical stark effect. *Journal of Physics B: Atomic and Molecular Physics*, 9(8):1199, 1976.
- [39] HJ Kimble and L Mandel. Theory of resonance fluorescence. *Physical Review A*, 13(6):2123, 1976.
- [40] Surendra Singh. Antibunching, sub-poissonian photon statistics and finite bandwidth effects in resonance fluorescence. *Optics Communications*, 44(4):254–258, 1983.
- [41] G. S. Agarwal. Time factorization of the higher-order intensity correlation functions in the theory of resonance fluorescence. *Phys. Rev. A*, 15:814–816, Feb 1977.